

---

# PETformer: Long-term Time Series Forecasting via Placeholder-enhanced Transformer

---

**Shengsheng Lin**

South China University of Technology  
linss2000@foxmail.com

**Weiwei Lin\***

South China University of Technology  
Peng Cheng Laboratory  
linww@scut.edu.cn

**Wentai Wu**

Peng Cheng Laboratory  
nnwtwu@pcl.ac.cn

**Songbo Wang**

South China University of Technology  
songbo1998@foxmail.com

**Yongxiang Wang**

South China University of Technology  
wangyxv@163.com

## Abstract

Recently, Transformer-based models have shown remarkable performance in long-term time series forecasting (LTSF) tasks due to their ability to model long-term dependencies. However, the validity of Transformers for LTSF tasks remains debatable, particularly since recent work has shown that simple linear models can outperform numerous Transformer-based approaches. This suggests that there are limitations to the application of Transformer in LTSF. Therefore, this paper investigates three key issues when applying Transformer to LTSF: temporal continuity, information density, and multi-channel relationships. Accordingly, we propose three innovative solutions, including Placeholder Enhancement Technique (PET), Long Sub-sequence Division (LSD), and Multi-channel Separation and Interaction (MSI), which together form a novel model called PETformer. These three key designs introduce prior biases suitable for LTSF tasks. Extensive experiments have demonstrated that PETformer achieves state-of-the-art (SOTA) performance on eight commonly used public datasets for LTSF, outperforming all other models currently available. This demonstrates that Transformer still possesses powerful capabilities in LTSF.

## 1 Introduction

Long-term time series forecasting (LTSF) highlights a wide range of applications across diverse fields such as transportation, weather, energy, and healthcare, and has remained a prominent topic in academic research for an extended period [37]. Owing to advancements in deep learning, mainstream LTSF methods have transitioned from traditional statistical approaches to deep learning-based techniques, including recurrent neural networks (RNNs) and convolutional neural networks (CNNs) [18]. Recently, Transformer-based models have achieved groundbreaking results in various deep learning fields [30, 19], and this trend has also extended to LTSF [37]. These models are particularly effective in capturing long-term dependencies in time series data, thereby pushing the boundaries of LTSF performance to new levels [38].

---

\*Corresponding author

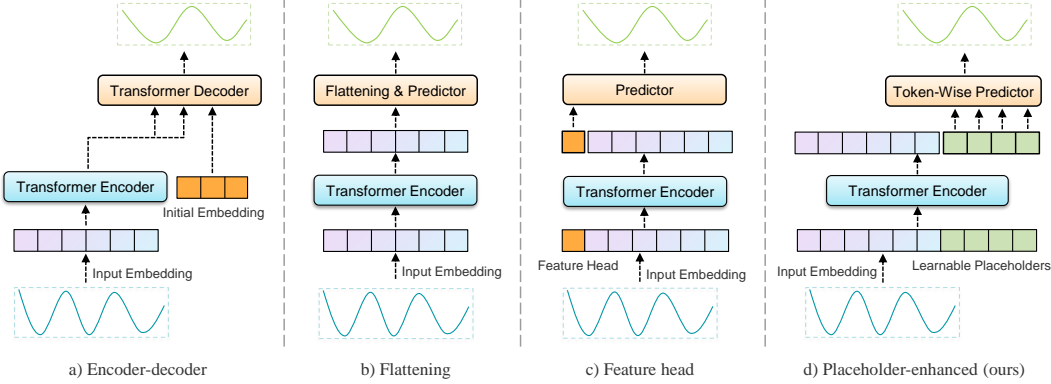


Figure 1: Comparison of different application techniques for Transformer in LTSF.

Despite attempts to encourage the use of Transformers in LTSF, their efficacy has been challenged by Dlinear [35], which attained unexpected results through a single-layer feedforward neural network, surpassing SOTA Transformer-based models. This finding suggests that there are still limitations in the current application of Transformer models in the LTSF domain. Given their impressive performance in Computer Vision (CV) [8] and Natural Language Processing (NLP) [5, 4], we ask: *what causes the performance gap between Transformer models in LTSF tasks and CV/NLP tasks?* This paper endeavors to investigate the following aspects and offer appropriate solutions:

**Temporal continuity** In contrast to CV/NLP tasks, LTSF tasks exhibit consistent and continuous temporal dependencies between input and output. The original Transformer encoder-decoder architecture was initially developed for NLP tasks, utilizing positional encoding and decoder recursion to maintain temporal relationships in the input and output, correspondingly. While contemporary Transformer-based LTSF models follow this architecture [37, 32, 38], recent studies indicate that the cross-attention mechanism between the encoder and decoder restricts the performance of LTSF [17]. Flattening and Feature Head are widely adopted techniques for feature extraction in CV/NLP [5, 21, 6, 28], both of which solely rely on the Transformer encoder and therefore do not utilize cross-attention mechanism. Recently, PatchTST [23] has utilized the Flattening technique and attained SOTA performance in LTSF, potentially due to the removal of temporal information loss caused by cross-attention. However, both Flattening and Feature Head fail to fully preserve temporal features as compressing excessive temporal information into a single constrained vector diminishes its richness, particularly for long-range future horizons. Consequently, we propose an innovative *Placeholder Enhancement Technique (PET)* that integrates full future data to be predicted alongside historical data as inputs to the Transformer model. Each placeholder represents a segment of future data to be predicted. This method allows the attention mechanism to directly model relationships between historical and future data, preserving temporal dependencies between inputs and outputs on a coherent temporal level while avoiding compression of temporal information at the output stage, as illustrated in Figure 1.

**Information density** Time series data, like images, is a low-density information source [10], contrasting with NLP where a single word carries rich semantics [5]. In time series data, only segments of sequences furnish adequate semantic information. ViT [6] divides images into  $16 \times 16$  sub-blocks for higher-level semantic information. Crossformer [36] and PatchTST [23] borrows this idea, dividing long sequences into patches, greatly improving Transformer performance in LTSF. We delve into longer sub-sequences, up to a length of 48, to leverage richer semantic information and achieve further improvements. The *Long Sub-sequence Division (LSD)* method addresses the considerable time complexity issue arising from the use of single points as inputs in prevalent Transformer-based models, simultaneously incorporating richer sub-sequence semantics to boost LTSF performance.

**Multi-channel relationships** In contrast to color images with static RGB channels, multivariate time series data (MTS) exhibits a variable number of channels characterized by intricate relationships. Existing Transformer-based models often mix data from multiple channels, predicting for all channels simultaneously [37, 32]. This method may disrupt the time sequence dependency information within

individual channels. DLinear introduced a channel separation design [35], which was later adopted by PatchTST [23]. However, this simple design did not account for inter-channel dependencies, which could potentially affect the model’s performance. In this paper, we delve deeper into diverse strategies for *Multi-channel Separation and Interaction (MSI)*, including inter-channel attention and channel identifiers. By employing channel interaction strategies after the independent extraction of time sequence features, interference between irrelevant channels can be substantially diminished during the model’s learning of sequence temporal dependencies.

In summary, this paper explores three key challenges in applying Transformer models to LTSF: temporal continuity, information density, and multi-channel relationships. We propose three key designs - PET, LSD, and MSI - to address these challenges and ultimately introduce a new solution called **PETformer**. Extensive experiments have demonstrated that PETformer achieves SOTA performance on eight commonly used public datasets for LTSF, outperforming all other currently available models, including both Transformer-based and non-Transformer-based models. Our work demonstrates that Transformer still possesses powerful capabilities in LTSF. We believe that the analysis and improvement methods presented in this paper will provide valuable references and inspirations for future research on time series tasks.

## 2 Related work

In the beginning, traditional statistical methods, including ARIMA [3] and VAR [12], were the primary approaches for time series prediction. As deep learning advanced, RNN-based methods (such as DeepAR [24], ConvLSTM [27] and LSTnet [15]) and CNN-based methods (such as TCN [1, 25] and Dilated CNN [34]) methods emerged. Nonetheless, RNN-based methods face limitations due to gradient explosion/forgetting issues, while CNN-based methods are constrained by their receptive fields and an inability to effectively model long-term dependencies. The Transformer model, leveraging the self-attention mechanism, inherently possesses the capacity to model long-term dependencies, as it can interact with all data simultaneously within a single operation [30]. However, when applied to LTSF, the original Transformer model suffers from high computational complexity. Numerous studies have concentrated on mitigating the complexity of Transformer in LTSF, including LogTrans [16], Longformer [2], Reformer [14], Informer [37], and Pyraformer [20]. Autoformer [32] introduced trend decomposition, which Fedformer [38] subsequently adopted and further combined with Fourier-enhanced technology.

Lately, the efficacy of Transformers in LTSF has been challenged by Dlinear [35], which employs simple single-layer neural networks and trend decomposition techniques. In response, Crossformer [36] and PatchTST [23] utilized patch techniques in CV [6, 22, 10] to effectively enhance the performance of Transformers in LTSF. Moreover, several remarkable non-Transformer-based models, including Micn [31], Film [39], and TimesNet [33], have recently surpassed the performance of numerous Transformer-based models.

## 3 Model architecture

The main architecture of PETformer, as depicted in Figure 2, takes input  $X = \{x_t^1, x_t^2, \dots, x_t^d\}_{t=1}^l$ , where  $l$  signifies the length of the historical look-back window. Initially, it separates  $X$  into  $d$  independent channel sequences, resulting in  $X' = \{X^1, X^2, \dots, X^d\}$ . Subsequently, the independent sequences  $X^i$  are partitioned into patches of length  $w$  and transformed into input embeddings, generating  $n$  tokens. These tokens are then input into the placeholder-enhanced Transformer encoder for feature extraction. This process yields  $m$  tokens for each independent sequence, amounting to a total of  $d \times m$  tokens after feature extraction from all  $d$  channels. The  $d \times m$  tokens are then transposed to obtain  $m \times d$  tokens, which undergo the inter-channel interaction module for inter-channel feature extraction. Finally, the tokens are fed into the token-wise predictor, which employs parameter-sharing linear layer for individual patch output prediction. After concatenation, the final output  $Y = \{y_t^1, y_t^2, \dots, y_t^d\}_{t=1}^h$  is obtained, where  $h$  refers to the length of the forecast horizon.

### 3.1 Sub-sequence division and tokenization

For the given historical data, each independent channel sequence  $X^i \in \mathbb{R}^l$  is divided into  $n$  sub-sequences  $X_{patched}^i \in \mathbb{R}^{n \times w}$ , where  $n$  is determined by the sub-sequence window length  $w$  and

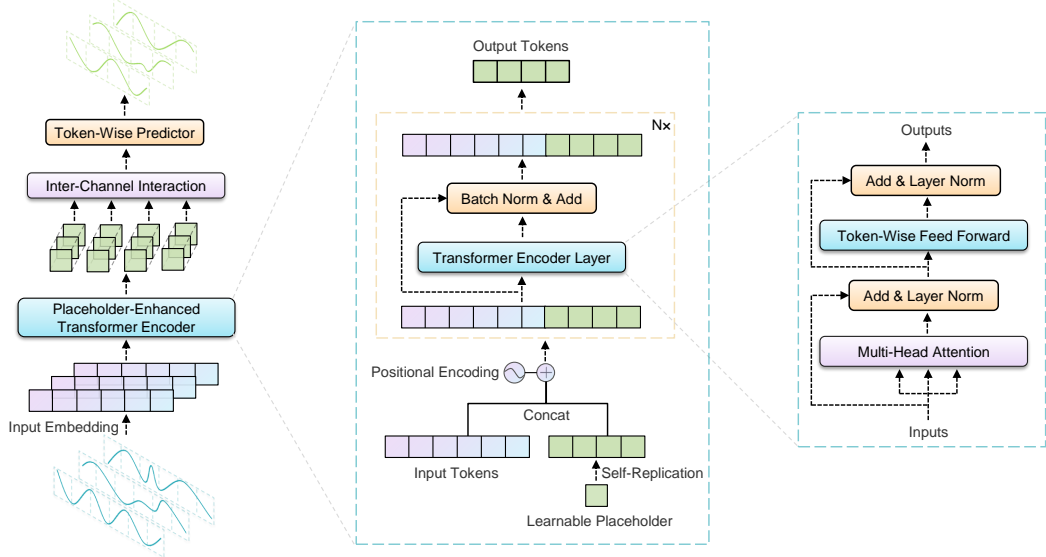


Figure 2: The PETformer model architecture.

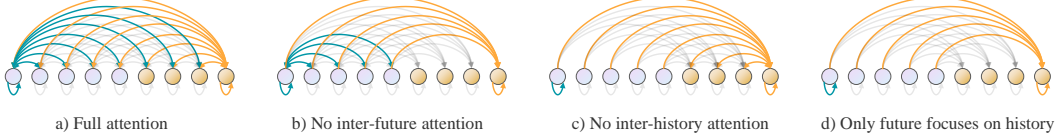


Figure 3: Different attention modes between history and future.

the stride length  $s$ , i.e.,  $n = \lfloor \frac{l-w}{s} + 1 \rfloor$ . Subsequently, each sub-sequence is mapped to a  $d_{model}$  dimensional vector through a parameter-sharing linear layer, resulting in  $X_{token}^i \in \mathbb{R}^{n \times d_{model}}$ .

For the future data to be predicted, the same tokenization strategy is employed. A learnable placeholder  $p \in \mathbb{R}^{d_{model}}$  is initially initialized, representing a future sub-sequence of length  $w$ . Subsequently, for a prediction horizon of  $h$  time steps,  $m$  placeholders are needed to represent the future, yielding  $Y_{token}^i \in \mathbb{R}^{m \times d_{model}}$ . In this case,  $m = \lfloor \frac{h-w}{s} + 1 \rfloor$ .

### 3.2 Placeholder-enhanced Transformer encoder

The placeholder-enhanced Transformer encoder takes an independent channel token sequence as input. Initially, a learnable placeholder is replicated  $m$  times and concatenated with the  $n$  tokens of input to form a sequence of  $n + m$  tokens, which is then augmented with position encoding. In this sequence, the first  $n$  tokens encompass historical data, while the last  $m$  tokens signify the future information to be learned, thereby facilitating direct interaction between historical and future information. The encoder contains  $N$  feature extraction blocks, wherein the token sequence in each block undergoes intra-channel token feature interaction through a single Transformer encoder layer, succeeded by batch normalization [11] and residual connection [9]. The Transformer encoder layer here is consistent with the vanilla Transformer [30]. Finally, the encoder outputs the last  $m$  tokens, which contain learned future prediction information.

Although the placeholders provide future-aware prior knowledge, they are not real future data, and whether more interaction should be done between historical data and placeholders is a question worth exploring. To this end, as shown in Figure 3, this work explores four different attention modes:

- **Full attention (FA):** This constitutes the standard operation, wherein bidirectional attention is conducted both within and between historical data and placeholders.
- **No inter-future attention (NIFA):** The information of the placeholder does not affect the interaction between real historical data, which means that the placeholder information is

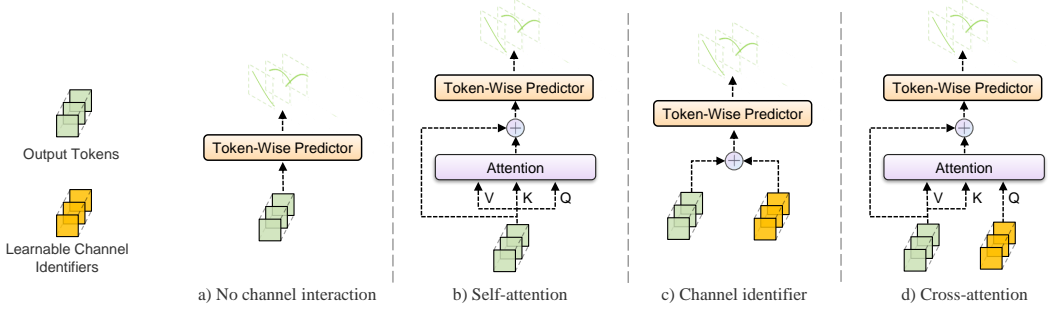


Figure 4: Different inter-channel interactions.

not provided to the outside, but it will obtain information from history. Historical data still interact with each other.

- **No inter-history attention (NIHA):** Conversely, historical data can be kept unchanged, allowing only placeholders to interact with each other and continuously learn future information from the existing historical data.
- **Only future focuses on history (OFFH):** This configuration combines both NIFA and NIHA modes, where each placeholder independently focuses on historical information.

### 3.3 Inter-channel interaction

Although Dlinear [35] and PatchTST [23] have demonstrated that the simple channel separation strategy is sufficient to achieve high-level performance, considering the inter-channel dependencies might prove advantageous in predicting future information for certain scenarios. Therefore, as shown in Figure 4, several ways to extract inter-channel features are explored in this work:

- **No channel interaction (NCI):** This method refrains from additional inter-channel interactions, solely capturing potential dependencies between channels through the shared parameters within the Placeholder-enhanced Transformer encoder.
- **Self-attention (SA):** Given the efficacy of the attention mechanism, utilizing self-attention to extract inter-channel features is a logical approach.
- **Channel identifier (CI):** Shao et al. [26] found that the lack of spatial distinguishability serves as a bottleneck when improving predictive performance in multivariate time series data. As a result, the channel identifier concept has been introduced as a substitute for complex spatial modeling in graph neural networks. This technique can be applied to differentiate among various channels in this study.
- **Cross-attention (CA):** The channel identifier distinguishes each unique channel. Naturally, it can serve as a query to pay attention to the temporal dependencies learned across multiple channels, thereby modeling the inter-channel dependencies.

### 3.4 Instance normalization and loss function

**Instance normalization** Besides the global preprocessing normalization of data, we also employ RevIN [13, 29] to tackle the distribution shift issue in time-series data between training and test sets. RevIN normalizes each individual sample prior to inputting it into the model and denormalizes it after obtaining the output from the model.

**Loss function** We utilize Smooth L1 loss [7], which amalgamates the advantages of both L1 loss and Mean Squared Error (MSE). This combined approach offers a more stable gradient, mitigating the likelihood of gradient explosion or decay during the training phase. In this work, the loss function is defined as follows:

$$\mathcal{L}(Y, \hat{Y}) = \frac{1}{d \cdot h} \sum_{t=1}^h \sum_{i=1}^d \rho_{\text{smooth}}(y_t^i - \hat{y}_t^i),$$

where

$$\rho_{\text{smooth}}(x) = \begin{cases} 0.5x^2 & \text{for } |x| < 1 \\ |x| - 0.5 & \text{otherwise.} \end{cases}$$

## 4 Experiments

In this section, we present the main results of PETformer on multivariate time series prediction tasks, as well as ablation experiments on the three key designs of our approach: PET, LSD, and MSI. Full details of these experiments and additional supplementary experiments are available in Appendix A due to the limitations of the main text length.

**Dataset** We conducted extensive experiments on eight widely used public datasets, including four ETT datasets (ETTh1, ETTh2, ETTm1, ETTm2) [37], Electricity, ILI, Weather, and Traffic [32], covering energy, transportation, medical, and weather domains. It should be noted that ETTh1, ETTh2, and ILI are small datasets, ETTm1, ETTm1, and Weather are medium datasets, and Electricity and Traffic are large datasets. Generally, smaller datasets contain more noise, while larger datasets exhibit more stable data distributions.

**Baselines and metrics** We choose SOTA and representative LTSF models as our baselines, comprising Transformer-based models like PatchTST [23], Crossformer [36], FEDformer [38], Autoformer [32], and Informer [37], in addition to non-Transformer-based models such as Dlinear [35] and Micn [31]. To assess the performance of these models, we employ widely used evaluation metrics: Mean Squared Error (MSE) and Mean Absolute Error (MAE). In every table presented throughout this paper, the top-performing results are emphasized in **bold**, whereas the runners-up are underlined.

### 4.1 Main results

Table 1 presents the outcomes of multivariate long-term forecasting. Overall, PETformer achieves SOTA performance on all prediction step settings for the eight datasets, outperforming all baseline methods. On average, compared to the most recent advanced model PatchTST, PETformer achieves a 4.7% MSE improvement and a 3.7% MAE improvement. Notably, for Dlinear, which has questioned the efficacy of Transformer in LTSF, PETformer achieves a 24.3% MSE improvement and a 14.9% MAE improvement. In terms of dataset size, for small datasets with a lot of noise, such as the ILI dataset, PETformer outperforms PatchTST with a 9% MSE improvement and a 5.2% MAE improvement, indicating that PETformer has stronger robustness in handling noisy data. For larger and more stable datasets where previous models have performed better, such as the Traffic dataset, PETformer still achieves a 1.3% MSE improvement and a 4.5% MAE improvement, indicating that PETformer can more stably capture the long-term dependencies in data.

Furthermore, in univariate prediction scenarios, even without inter-channel interaction, PETformer still achieves the best performance on the ETT completion dataset, outperforming all baselines. On average, compared to PatchTST, PETformer achieves a 4.9% MSE improvement and a 2.3% MAE improvement. This demonstrates that the PET and LSD designs indeed bring more useful prior knowledge to univariate time series prediction tasks. The full results of univariate time series prediction can be found in Appendix A.2.

### 4.2 Ablation studies

We conducted ablation experiments on three datasets of varying scales and numbers of variables (ETTh1, Weather, and Traffic) to thoroughly assess the effectiveness of the proposed methods.

#### 4.2.1 Placeholder enhancement technique

Table 2 presents the outcomes of the ablation study for PET. The native Encoder-Decoder architecture in the Transformer yields the poorest performance, corroborating that cross self-attention may lead to the loss of temporal dependency transmission in LTSF [17]. The Flattening technique substantially enhances Transformer performance, aligning with observations in PatchTST [23]. Although, to the best of our knowledge, the Feature Head technique has not been applied in the LTSF domain, our research indicates that its performance surpasses the Flattening technique. As anticipated, our

Table 1: Multivariate long-term series forecasting results. PETformer employs a look-back window length of  $l = 72$  for the ILI dataset and  $l = 720$  for the remaining datasets. It should be noted that other models typically perform optimally with different look-back window lengths. To avoid underestimating their performance, we conducted additional experiments with the other models using look-back window lengths of  $l \in \{24, 48, 72, 144\}$  for the ILI dataset and  $l \in \{96, 192, 336, 720\}$  for the other datasets, and the best result from these experiments was selected as their final outcome.

Models		PETformer (ours)		PatchTST (2023)		Dlinear (2023)		MICN (2023)		Crossformer (2023)		FEDformer* (2022)		Autoformer* (2021)		Informer* (2021)	
Metric		MSE	MAE	MSE	MAE	MSE	MAE	MSE	MAE	MSE	MAE	MSE	MAE	MSE	MAE	MSE	MAE
ETTh1	96	<b>0.347</b>	<b>0.377</b>	0.376	0.408	0.378	0.402	0.404	0.429	0.380	0.419	0.376	0.415	0.435	0.446	0.941	0.769
	192	<b>0.390</b>	<b>0.404</b>	0.416	0.423	0.415	0.425	0.475	0.484	0.419	0.445	0.423	0.446	0.456	0.457	1.007	0.786
	336	<b>0.419</b>	<b>0.418</b>	0.425	0.440	0.447	0.448	0.482	0.489	0.438	0.451	0.444	0.462	0.486	0.487	1.038	0.784
	720	<b>0.437</b>	<b>0.449</b>	0.448	0.470	0.480	0.489	0.599	0.576	0.508	0.514	0.469	0.492	0.515	0.517	1.144	0.857
ETTh2	96	<b>0.272</b>	<b>0.329</b>	0.275	0.338	0.282	0.346	0.289	0.354	0.383	0.420	0.332	0.374	0.332	0.368	1.549	0.952
	192	<b>0.338</b>	<b>0.374</b>	0.338	0.378	0.350	0.396	0.408	0.444	0.421	0.450	0.407	0.446	0.426	0.434	3.792	1.542
	336	<b>0.328</b>	<b>0.380</b>	0.329	<b>0.380</b>	0.410	0.437	0.547	0.516	0.449	0.459	0.4	0.447	0.477	0.479	4.215	1.642
	720	0.401	0.439	<b>0.379</b>	<b>0.422</b>	0.587	0.544	0.834	0.688	0.472	0.497	0.412	0.469	0.453	0.490	3.656	1.619
ETTm1	96	<b>0.282</b>	<b>0.325</b>	0.293	0.342	0.306	0.345	0.301	0.352	0.295	0.350	0.326	0.390	0.51	0.492	0.626	0.560
	192	<b>0.318</b>	<b>0.349</b>	0.328	0.365	0.335	0.365	0.344	0.380	0.339	0.381	0.365	0.415	0.514	0.495	0.725	0.619
	336	<b>0.348</b>	<b>0.372</b>	0.362	0.394	0.373	0.391	0.379	0.401	0.419	0.432	0.392	0.425	0.51	0.492	1.005	0.741
	720	<b>0.404</b>	<b>0.403</b>	0.414	0.420	0.422	0.422	0.429	0.429	0.579	0.551	0.446	0.458	0.527	0.493	1.133	0.845
ETTm2	96	<b>0.160</b>	<b>0.248</b>	0.163	0.255	0.164	0.259	0.177	0.274	0.296	0.352	0.18	0.271	0.205	0.293	0.355	0.462
	192	<b>0.217</b>	<b>0.288</b>	0.221	0.292	0.233	0.314	0.236	0.310	0.342	0.385	0.252	0.318	0.278	0.336	0.595	0.586
	336	0.274	<b>0.326</b>	<b>0.270</b>	0.329	0.291	0.355	0.299	0.350	0.410	0.425	0.324	0.364	0.343	0.379	1.27	0.871
	720	<b>0.345</b>	<b>0.376</b>	0.347	0.378	0.407	0.433	0.421	0.434	0.563	0.538	0.41	0.420	0.414	0.419	3.001	1.267
Electricity	96	<b>0.128</b>	<b>0.220</b>	0.130	0.223	0.133	0.230	0.151	0.260	0.198	0.292	0.186	0.302	0.196	0.313	0.304	0.393
	192	<b>0.144</b>	<b>0.236</b>	0.147	0.240	0.147	0.244	0.165	0.276	0.266	0.330	0.197	0.311	0.211	0.324	0.327	0.417
	336	<b>0.159</b>	<b>0.252</b>	0.164	0.257	0.162	0.261	0.183	0.291	0.343	0.377	0.213	0.328	0.214	0.327	0.333	0.422
	720	<b>0.195</b>	<b>0.286</b>	0.203	0.292	0.196	0.294	0.201	0.312	0.398	0.422	0.233	0.344	0.236	0.342	0.351	0.427
ILI	24	<b>1.204</b>	<b>0.687</b>	1.356	0.732	2.000	0.987	2.483	1.058	3.217	1.198	2.624	1.095	2.906	1.182	4.657	1.449
	36	1.246	0.709	<b>1.244</b>	<b>0.705</b>	2.202	1.026	2.370	0.987	3.136	1.199	2.516	1.021	2.585	1.038	4.65	1.463
	48	<b>1.446</b>	<b>0.760</b>	1.604	0.791	2.278	1.059	2.371	1.007	3.331	1.236	2.505	1.041	3.024	1.145	5.004	1.542
	60	<b>1.430</b>	<b>0.774</b>	1.648	0.860	2.478	1.111	2.513	1.055	3.609	1.265	2.742	1.122	2.761	1.114	5.071	1.543
Traffic	96	<b>0.357</b>	<b>0.240</b>	0.367	0.253	0.385	0.269	0.445	0.295	0.487	0.274	0.576	0.359	0.597	0.371	0.733	0.410
	192	<b>0.376</b>	<b>0.248</b>	0.382	0.259	0.395	0.273	0.461	0.302	0.497	0.279	0.61	0.380	0.607	0.382	0.777	0.435
	336	<b>0.392</b>	<b>0.255</b>	0.396	0.267	0.409	0.281	0.483	0.307	0.517	0.285	0.608	0.375	0.623	0.387	0.776	0.434
	720	<b>0.430</b>	<b>0.276</b>	0.433	0.287	0.449	0.305	0.527	0.310	0.584	0.323	0.621	0.375	0.639	0.395	0.827	0.466
Weather	96	0.146	<b>0.186</b>	0.147	0.198	0.169	0.231	0.167	0.231	<b>0.144</b>	0.208	0.238	0.314	0.249	0.329	0.354	0.405
	192	<b>0.190</b>	<b>0.229</b>	<b>0.190</b>	0.241	0.213	0.273	0.212	0.271	0.192	0.263	0.275	0.329	0.325	0.370	0.419	0.434
	336	<b>0.241</b>	<b>0.271</b>	0.243	0.284	0.260	0.314	0.275	0.337	0.246	0.306	0.339	0.377	0.351	0.391	0.583	0.543
	720	0.314	0.323	<b>0.305</b>	0.328	0.315	0.353	<b>0.312</b>	0.349	0.318	0.361	0.389	0.409	0.415	0.426	0.916	0.705
Avg.		<b>0.427</b>	<b>0.369</b>	0.448	0.383	0.565	0.434	0.623	0.455	0.756	0.490	0.651	0.472	0.713	0.497	1.629	0.825

\* denotes that the data originates from PatchTST [23], where the experimental reproduction strategy aligns consistently with this work.

PET approach achieves the best results, regardless of the attention mode in PET, demonstrating the superiority of the PET method. Furthermore, the Full Attention (FA) mode outperforms the other three modes, indirectly substantiating that allowing more historical and future data to interact directly at the same level of attention is advantageous.

#### 4.2.2 Long sub-sequence division

Table 3 presents the outcomes of the ablation study for LSD. The point-wise attention approach, despite being the mainstream Transformer-based application method, yielded the poorest performance. In contrast, our LSD approach demonstrated significantly better results. Notably, as the window size of the sub-sequence incrementally increased, the LTSF performance continued to improve. This suggests that larger window sub-sequence divisions provide richer semantic information within our framework, directly influencing the LTSF performance. Although the performance improvement due to the growth of  $w$  has not yet saturated, larger values of  $w$  cannot be explored in this work since  $w = 48$  is already the greatest common divisor of  $h \in \{96, 192, 336, 720\}$ .

Additionally, it has been noted that employing point-wise input on sizable datasets, such as Traffic, results in out-of-memory issues, owing to the exponential increase in complexity inherent to the original Transformer model. In our work, while we refrained from adopting sparse self-attention to decrease complexity, we effectively reduced complexity by devising an extensive sub-sequence window length, as demonstrated in Table 4. In PETformer, we set the default values as  $l = 720$ ,  $w = 48$  (in contrast, PatchTST employs a default window length of  $w = 16$ ), and  $h \in \{96, 192, 336, 720\}$ , yielding the lowest complexity among these Transformer-based models.

Table 2: Ablation study of the PET. Various application techniques for Transformer, as depicted in Figure 1, are incorporated. In the case of PET, we evaluated different attention modes between historical and future data, as illustrated in Figure 3.

Models		Enc-dec		Flattening		Feature Head		PET/FA <sup>†</sup>		PET/NIFA		PET/NIHA		PET/OFFH	
Metric		MSE	MAE	MSE	MAE	MSE	MAE	MSE	MAE	MSE	MAE	MSE	MAE	MSE	MAE
ETTh1	96	0.399	0.409	0.377	0.402	0.350	0.382	0.348	0.379	<b>0.347</b>	<b>0.378</b>	0.352	0.381	0.349	0.379
	192	0.435	0.439	0.416	0.427	0.391	0.408	0.389	<b>0.403</b>	0.390	0.403	<b>0.388</b>	0.403	0.390	0.403
	336	0.472	0.456	0.449	0.447	0.425	0.434	<b>0.419</b>	0.420	<b>0.422</b>	<b>0.419</b>	0.425	0.422	0.425	0.421
	720	0.513	0.496	0.469	0.476	0.445	0.462	<b>0.435</b>	<b>0.447</b>	0.450	0.456	<b>0.443</b>	<b>0.453</b>	0.453	0.457
Weather	96	0.196	0.257	<b>0.145</b>	0.189	0.145	0.186	0.145	<b>0.184</b>	0.145	0.185	0.147	0.186	0.147	0.187
	192	0.239	0.289	0.193	0.235	0.191	0.231	<b>0.190</b>	<b>0.228</b>	0.190	0.229	0.191	0.230	0.191	0.230
	336	0.299	0.331	0.245	0.278	0.242	0.273	<b>0.241</b>	<b>0.270</b>	0.241	<b>0.270</b>	0.242	0.271	<b>0.241</b>	0.270
	720	0.371	0.388	0.323	0.334	0.318	0.328	0.312	<b>0.322</b>	0.314	0.323	<b>0.311</b>	0.322	<b>0.311</b>	<b>0.322</b>
<b>Avg.</b>		0.386	0.361	0.351	0.322	0.343	0.317	<b>0.337</b>	<b>0.308</b>	0.339	0.309	0.341	0.312	0.342	0.312

† denotes the default mode in this work.

Table 3: Ablation study of the LSD. A comparison of performance between using single points and sub-sequences as input granularity is presented. For the LSD, various window lengths  $w \in \{6, 12, 24, 48\}$  are evaluated. The '-' symbol denotes out-of-memory issues encountered in our experimental environment.

Models		Point		LSD/w=6		LSD/w=12		LSD/w=24		LSD/w=48 <sup>†</sup>	
Metric		MSE	MAE	MSE	MAE	MSE	MAE	MSE	MAE	MSE	MAE
ETTh1	96	0.910	0.424	0.435	0.424	0.361	0.390	0.349	0.380	<b>0.347</b>	<b>0.377</b>
	192	0.920	0.472	<b>0.517</b>	0.472	0.406	0.416	<b>0.392</b>	<b>0.405</b>	<b>0.390</b>	<b>0.404</b>
	336	0.815	0.539	0.636	0.539	0.435	0.430	0.424	<b>0.425</b>	<b>0.419</b>	<b>0.418</b>
	720	0.832	0.604	0.719	0.604	0.461	0.468	<b>0.456</b>	<b>0.458</b>	<b>0.437</b>	<b>0.449</b>
Weather	96	0.159	0.202	0.159	0.200	0.149	0.189	0.146	0.186	<b>0.146</b>	<b>0.186</b>
	192	0.206	0.243	0.206	0.244	0.193	0.233	<b>0.189</b>	0.229	0.190	<b>0.229</b>
	336	0.255	0.289	0.256	0.284	0.244	0.274	<b>0.241</b>	0.271	0.241	<b>0.271</b>
	720	0.323	0.333	0.326	0.340	0.315	0.327	<b>0.312</b>	0.324	0.314	<b>0.323</b>
Traffic	96	-	-	0.437	0.316	0.378	0.251	0.365	0.243	<b>0.357</b>	<b>0.240</b>
	192	-	-	0.485	0.356	0.392	0.257	<b>0.382</b>	0.250	<b>0.376</b>	<b>0.248</b>
	336	-	-	0.492	0.345	0.413	0.270	<b>0.397</b>	0.258	<b>0.392</b>	<b>0.255</b>
	720	-	-	0.485	0.327	0.483	0.326	<b>0.435</b>	0.278	<b>0.430</b>	<b>0.276</b>
<b>Avg.</b>		-	-	0.429	0.371	0.352	0.319	0.341	0.309	<b>0.337</b>	<b>0.306</b>

† denotes the default mode in this work.

#### 4.2.3 Multi-channel separation and interaction

Table 5 presents the outcomes of the ablation study for MSI. Though DCM is the prevalent method for current Transformer-based models, it yielded the poorest performance in our experiments, substantiating that the DCM approach might severely disrupt intra-channel temporal dependencies. Conversely, the MSI-based method attained substantial performance enhancements. Overall, the four MSI approaches demonstrated minimal differences; however, we observed that the no channel interaction (NCI) mode offered a minor advantage, prompting further consideration. We postulate

Table 4: Computational complexity per layer of Transformer-based models, with  $l$  denoting the length of the historical look-back window,  $w$  signifying the sub-sequence window length, and  $h$  representing the length of the forecast horizon.

Models	Computation complexity
Transformer [30]	$O(l^2)$
Informer [37]	$O(l \log l)$
Fedformer [38]	$O(l)$
PatchTST [23]	$O((\frac{l}{w})^2)$
PETformer (ours)	$O((\frac{l+h}{w})^2)$

Table 5: Ablation study of the MSI. The direct channel mixing (DCM) approach is compared with the MSI approach. For the MSI method, various strategies illustrated in Figure 4 are evaluated.

Models	DCM	MSI/NCI		MSI/SA <sup>†</sup>		MSI/CI		MSI/CA	
		MSE	MAE	MSE	MAE	MSE	MAE	MSE	MAE
ETTh1	96	0.409	0.435	0.348	0.379	<b>0.348</b>	0.379	0.349	0.378
	192	0.470	0.476	<u>0.389</u>	0.403	<b>0.389</b>	<b>0.403</b>	0.394	0.407
	336	0.512	0.503	<u>0.419</u>	0.419	0.419	0.420	<b>0.415</b>	<b>0.417</b>
	720	0.626	0.574	<u>0.444</u>	<u>0.452</u>	<b>0.435</b>	<b>0.447</b>	0.454	0.458
Weather	96	0.147	0.195	<u>0.145</u>	0.185	0.145	<b>0.184</b>	0.145	<b>0.144</b>
	192	0.198	0.245	<u>0.189</u>	<b>0.228</b>	0.189	<u>0.228</u>	<b>0.188</b>	0.229
	336	0.255	0.291	0.241	<b>0.270</b>	<u>0.241</u>	<u>0.270</u>	0.242	<b>0.272</b>
	720	0.321	0.340	0.315	0.323	<u>0.313</u>	<u>0.322</u>	<b>0.311</b>	<b>0.322</b>
Avg.		0.758	0.464	0.337	<b>0.307</b>	<b>0.337</b>	0.308	0.338	0.308
0.341 0.311									

<sup>†</sup> denotes the default mode in this work.

that this occurs due to MTS displaying a varying number of channels, resulting in intricate and challenging-to-estimate inter-channel relationships. For example, in ETTH1, containing only 7 variables, inter-channel interaction can yield improvement; conversely, for Traffic, with its 862 variables, the inter-channel relationships become too complex for the model to handle. Nevertheless, although the diverse inter-channel interaction methods did not demonstrate considerable enhancement compared to NCI, these results indicate potential directions for future research in effectively modeling the complex relationships among multivariate channels.

## 5 Discussion

In this section, we systematically discuss the reasons behind PETformer’s improved effectiveness in LTSF. We believe that PETformer introduces more prior biases suitable for LTSF tasks, which can be summarized as follows:

- The PET design introduces a future-aware bias. On one hand, it places real historical data and the future data to be predicted at the same level, allowing for a more direct modeling of the relationship between the past and future while maintaining coherent temporal continuity. On the other hand, for long-term prediction tasks, an excessively long prediction horizon may cause the model to lose accurate cognition of time. The PET design precisely places position encoding on each future window, enabling the model to have a more accurate time concept.
- The LSD design incorporates a bias for combining long and short-term dependencies. On one hand, the larger window design provides more semantic richness and a longer view of historical data, as the same number of tokens can reveal information further into the past. On the other hand, this design enables the Transformer to learn short-term dependencies within a single token and long-term dependencies across tokens, with the combination of the two leading to improved performance.
- The MSI design introduces a bias towards more important temporal dependencies. This allows the model to focus more on extracting temporal dependency features in the time domain, which is often crucial for accurate predictions. Furthermore, channel separation augments the sample count, consequently bolstering the model’s capacity to generalize and forecast individual channels. This finding is further elaborated upon in Appendix A.3.

## 6 Conclusion

This paper investigates the factors leading to the Transformer’s subpar performance in the LTSF domain, considering three potential perspectives: temporal continuity, information density, and multi-channel relationships. We introduce three key designs - PET, LSD, and MSI - to tackle these

challenges, collectively forming our comprehensive solution, PETformer. Experimental outcomes from eight public datasets illustrate that PETformer surpasses existing models, attaining SOTA performance. Thorough and meticulous ablation experiments reveal that the three designs proposed in this paper play a crucial role in enhancing Transformer’s performance in LTSF. We carry out a systematic analysis of the factors contributing to PETformer’s success and posit that these insights could provide valuable guidance and inspiration for future research in time series tasks.

## References

- [1] Shaojie Bai, J Zico Kolter, and Vladlen Koltun. An empirical evaluation of generic convolutional and recurrent networks for sequence modeling. *arXiv preprint arXiv:1803.01271*, 2018.
- [2] Iz Beltagy, Matthew E Peters, and Arman Cohan. Longformer: The long-document transformer. *arXiv preprint arXiv:2004.05150*, 2020.
- [3] George EP Box and David A Pierce. Distribution of residual autocorrelations in autoregressive-integrated moving average time series models. *Journal of the American statistical Association*, 65(332):1509–1526, 1970.
- [4] Tom Brown, Benjamin Mann, Nick Ryder, Melanie Subbiah, Jared D Kaplan, Prafulla Dhariwal, Arvind Neelakantan, Pranav Shyam, Girish Sastry, Amanda Askell, Sandhini Agarwal, Ariel Herbert-Voss, Gretchen Krueger, Tom Henighan, Rewon Child, Aditya Ramesh, Daniel Ziegler, Jeffrey Wu, Clemens Winter, Chris Hesse, Mark Chen, Eric Sigler, Mateusz Litwin, Scott Gray, Benjamin Chess, Jack Clark, Christopher Berner, Sam McCandlish, Alec Radford, Ilya Sutskever, and Dario Amodei. Language models are few-shot learners. In *Advances in Neural Information Processing Systems (NeurIPS)*, 2020.
- [5] Jacob Devlin, Ming-Wei Chang, Kenton Lee, and Kristina Toutanova. Bert: Pre-training of deep bidirectional transformers for language understanding. *arXiv preprint arXiv:1810.04805*, 2018.
- [6] Alexey Dosovitskiy, Lucas Beyer, Alexander Kolesnikov, Dirk Weissenborn, Xiaohua Zhai, Thomas Unterthiner, Mostafa Dehghani, Matthias Minderer, Georg Heigold, Sylvain Gelly, et al. An image is worth 16x16 words: Transformers for image recognition at scale. *arXiv preprint arXiv:2010.11929*, 2020.
- [7] Ross Girshick. Fast r-cnn. In *Proceedings of the IEEE international conference on computer vision (ICCV)*, pages 1440–1448, 2015.
- [8] Kai Han, Yunhe Wang, Hanting Chen, Xinghao Chen, Jianyuan Guo, Zhenhua Liu, Yehui Tang, An Xiao, Chunjing Xu, Yixing Xu, et al. A survey on vision transformer. *IEEE transactions on pattern analysis and machine intelligence*, 45(1):87–110, 2022.
- [9] Kaiming He, Xiangyu Zhang, Shaoqing Ren, and Jian Sun. Deep residual learning for image recognition. In *Proceedings of the IEEE/CVF Conference on Computer Vision and Pattern Recognition (CVPR)*, pages 770–778, 2016.
- [10] Kaiming He, Xinlei Chen, Saining Xie, Yanghao Li, Piotr Dollár, and Ross Girshick. Masked autoencoders are scalable vision learners. In *Proceedings of the IEEE/CVF Conference on Computer Vision and Pattern Recognition (CVPR)*, pages 16000–16009, 2022.
- [11] Sergey Ioffe and Christian Szegedy. Batch normalization: Accelerating deep network training by reducing internal covariate shift. In *International Conference on Machine Learning (ICML)*, pages 448–456, 2015.
- [12] Lutz Kilian and Helmut Lütkepohl. *Structural vector autoregressive analysis*. Cambridge University Press, 2017.
- [13] Taesung Kim, Jinhee Kim, Yunwon Tae, Cheonbok Park, Jang-Ho Choi, and Jaegul Choo. Reversible instance normalization for accurate time-series forecasting against distribution shift. In *International Conference on Learning Representations (ICLR)*, 2021.

[14] Nikita Kitaev, Łukasz Kaiser, and Anselm Levskaya. Reformer: The efficient transformer. *arXiv preprint arXiv:2001.04451*, 2020.

[15] Guokun Lai, Wei-Cheng Chang, Yiming Yang, and Hanxiao Liu. Modeling long-and short-term temporal patterns with deep neural networks. In *The 41st international ACM SIGIR conference on research & development in information retrieval*, pages 95–104, 2018.

[16] Shiyang Li, Xiaoyong Jin, Yao Xuan, Xiyou Zhou, Wenhui Chen, Yu-Xiang Wang, and Xifeng Yan. Enhancing the locality and breaking the memory bottleneck of transformer on time series forecasting. In *Advances in Neural Information Processing Systems (NeurIPS)*, 2019.

[17] Zhe Li, Zhongwen Rao, Lujia Pan, and Zenglin Xu. Mts-mixers: Multivariate time series forecasting via factorized temporal and channel mixing. *arXiv preprint arXiv:2302.04501*, 2023.

[18] Bryan Lim and Stefan Zohren. Time-series forecasting with deep learning: a survey. *Philosophical Transactions of the Royal Society A*, 379(2194):20200209, 2021.

[19] Tianyang Lin, Yuxin Wang, Xiangyang Liu, and Xipeng Qiu. A survey of transformers. *AI Open*, 3:111–132, 2022. ISSN 2666-6510. doi: <https://doi.org/10.1016/j.aiopen.2022.10.001>. URL <https://www.sciencedirect.com/science/article/pii/S2666651022000146>.

[20] Shizhan Liu, Hang Yu, Cong Liao, Jianguo Li, Weiyao Lin, Alex X Liu, and Schahram Dustdar. Pyraformer: Low-complexity pyramidal attention for long-range time series modeling and forecasting. In *International Conference on Learning Representations (ICLR)*, 2021.

[21] Yinhan Liu, Myle Ott, Naman Goyal, Jingfei Du, Mandar Joshi, Danqi Chen, Omer Levy, Mike Lewis, Luke Zettlemoyer, and Veselin Stoyanov. Roberta: A robustly optimized bert pretraining approach. *arXiv preprint arXiv:1907.11692*, 2019.

[22] Ze Liu, Yutong Lin, Yue Cao, Han Hu, Yixuan Wei, Zheng Zhang, Stephen Lin, and Baining Guo. Swin transformer: Hierarchical vision transformer using shifted windows. In *Proceedings of the IEEE/CVF international conference on computer vision*, pages 10012–10022, 2021.

[23] Yuqi Nie, Nam H Nguyen, Phanwadee Sinthong, and Jayant Kalagnanam. A time series is worth 64 words: Long-term forecasting with transformers. In *International Conference on Learning Representations (ICLR)*, 2023.

[24] David Salinas, Valentin Flunkert, Jan Gasthaus, and Tim Januschowski. Deepar: Probabilistic forecasting with autoregressive recurrent networks. *International Journal of Forecasting*, 36(3): 1181–1191, 2020.

[25] Rajat Sen, Hsiang-Fu Yu, and Inderjit S Dhillon. Think globally, act locally: A deep neural network approach to high-dimensional time series forecasting. In *Advances in Neural Information Processing Systems (NeurIPS)*, 2019.

[26] Zezhi Shao, Zhao Zhang, Fei Wang, Wei Wei, and Yongjun Xu. Spatial-temporal identity: A simple yet effective baseline for multivariate time series forecasting. In *Proceedings of the 31st ACM International Conference on Information & Knowledge Management (CIKM)*, pages 4454–4458, 2022.

[27] Xingjian SHI, Zhourong Chen, Hao Wang, Dit-Yan Yeung, Wai-kin Wong, and Wang-chun WOO. Convolutional lstm network: A machine learning approach for precipitation nowcasting. In *Advances in Neural Information Processing Systems (NeurIPS)*, volume 28, 2015.

[28] Hugo Touvron, Matthieu Cord, Matthijs Douze, Francisco Massa, Alexandre Sablayrolles, and Hervé Jégou. Training data-efficient image transformers & distillation through attention. In *International Conference on Machine Learning (ICML)*, pages 10347–10357, 2021.

[29] Dmitry Ulyanov, Andrea Vedaldi, and Victor Lempitsky. Instance normalization: The missing ingredient for fast stylization. *arXiv preprint arXiv:1607.08022*, 2016.

[30] Ashish Vaswani, Noam Shazeer, Niki Parmar, Jakob Uszkoreit, Llion Jones, Aidan N Gomez, Łukasz Kaiser, and Illia Polosukhin. Attention is all you need. In *Advances in Neural Information Processing Systems (NeurIPS)*, volume 30, 2017.

- [31] Huiqiang Wang, Jian Peng, Feihu Huang, Jince Wang, Junhui Chen, and Yifei Xiao. MICN: Multi-scale local and global context modeling for long-term series forecasting. In *International Conference on Learning Representations (ICLR)*, 2023.
- [32] Haixu Wu, Jiehui Xu, Jianmin Wang, and Mingsheng Long. Autoformer: Decomposition transformers with auto-correlation for long-term series forecasting. In *Advances in Neural Information Processing Systems (NeurIPS)*, 2021.
- [33] Haixu Wu, Tengge Hu, Yong Liu, Hang Zhou, Jianmin Wang, and Mingsheng Long. Timesnet: Temporal 2d-variation modeling for general time series analysis. In *International Conference on Learning Representations (ICLR)*, 2023.
- [34] Fisher Yu and Vladlen Koltun. Multi-scale context aggregation by dilated convolutions. *arXiv preprint arXiv:1511.07122*, 2015.
- [35] Ailing Zeng, Muxi Chen, Lei Zhang, and Qiang Xu. Are transformers effective for time series forecasting? In *Proceedings of the AAAI Conference on Artificial Intelligence (AAAI)*, 2023.
- [36] Yunhao Zhang and Junchi Yan. Crossformer: Transformer utilizing cross-dimension dependency for multivariate time series forecasting. In *International Conference on Learning Representations (ICLR)*, 2023.
- [37] Haoyi Zhou, Shanghang Zhang, Jieqi Peng, Shuai Zhang, Jianxin Li, Hui Xiong, and Wancai Zhang. Informer: Beyond efficient transformer for long sequence time-series forecasting. In *Proceedings of the AAAI conference on artificial intelligence (AAAI)*, 2021.
- [38] Tian Zhou, Ziqing Ma, Qingsong Wen, Xue Wang, Liang Sun, and Rong Jin. Fedformer: Frequency enhanced decomposed transformer for long-term series forecasting. In *International Conference on Machine Learning (ICML)*, 2022.
- [39] Tian Zhou, Ziqing Ma, xue wang, Qingsong Wen, Liang Sun, Tao Yao, Wotao Yin, and Rong Jin. FiLM: Frequency improved legendre memory model for long-term time series forecasting. In *Advances in Neural Information Processing Systems (NeurIPS)*, 2022.

## A Appendix

In this section, we present the experimental details of PETformer and provide additional supportive experiments to further demonstrate its effectiveness. The organization of this section is as follows:

- Appendix A.1 provides details on the datasets, baselines, experimental parameters, and environments used in the experiments.
- Appendix A.2 presents the complete results of the univariate forecasting experiments.
- Appendix A.3 discusses the effect of channel separation on the model’s ability to predict individual channels.
- Appendix A.4 investigates the impact of the look-back window length on model performance.
- Appendix A.5 provides the complete reproducible experiment results of baselines.
- Appendix A.6 presents the results of the robustness experiments conducted to assess the model’s stability to random seed perturbations.
- Appendix A.7 showcases the results on the large datasets to demonstrate the model’s predictive ability.

### A.1 Experimental details

#### A.1.1 Datasets

Table 6: Summary of Dataset Characteristics

Datasets	ETTh1	ETTh2	ETTm1	ETTm2	Electricity	ILI	Traffic	Weather
Dimension	7	7	7	7	321	7	862	21
Frequency	1 hour	1 hour	15 min	15 min	1 hour	7 day	1 hour	10 min
Length	17420	17420	69680	69680	26304	966	52696	52696

We use the most popular multivariate datasets in LTSF, including ETT<sup>2</sup> (ETTh1, ETTh2, ETTm1, ETTm2), Electricity<sup>3</sup>, ILI<sup>4</sup>, Traffic<sup>5</sup>, and Weather<sup>6</sup>. These datasets encompass various domains, such as energy, healthcare, transportation, and weather. Table 6 presents key characteristics of the eight datasets. The dimensions of each dataset range from 7 to 862, with frequencies ranging from 10 minutes to 7 days. The length of the datasets varies from 966 to 69,680 data points. We split all datasets into training, validation, and test sets in chronological order, using a ratio of 6:2:2 for the ETT dataset and 7:1:2 for the remaining datasets. For a more detailed discussion on the datasets, we recommend referring to the Autoformer paper [32].

#### A.1.2 Baselines

We choose SOTA and the most representative LTSF models as our baselines, including both Transformer-based and non-Transformer-based models, as follows:

- PatchTST [23]: the current SOTA LTSF model as of April 2023. It utilizes channel-independent and patch techniques and achieves the highest performance by utilizing the native Transformer.
- Dlinear [35]: a highly insightful work that employs simple linear models and trend decomposition techniques, outperforming all Transformer-based models at the time. This work inspired us to reflect on the utility of Transformers in LTSF and indirectly led to the birth of PETformer in our study.

<sup>2</sup><https://github.com/zhouhaoyi/ETDataset>

<sup>3</sup><https://archive.ics.uci.edu/ml/datasets/ElectricityLoadDiagrams20112014>

<sup>4</sup><https://gis.cdc.gov/grasp/fluvview/fluportaldashboard.html>

<sup>5</sup><https://pems.dot.ca.gov/>

<sup>6</sup><https://www.bgc-jena.mpg.de/wetter/>

- Micn [31]: another non-Transformer model that enhances the performance of CNN models in LTSF through down-sampled convolution and isometric convolution, outperforming many Transformer-based models. This excellent work has been selected for oral presentation at ICLR 2023.
- Crossformer [36]: similar to PatchTST, it utilizes the patch technique commonly used in the CV domain. However, unlike PatchTST’s independent channel design, it leverages cross-dimension dependency to enhance LTSF performance. This outstanding work has also been selected for oral presentation at ICLR 2023.
- FEDformer [38]: it employs trend decomposition and Fourier transformation techniques to improve the performance of Transformer-based models in LTSF. It was the best-performing Transformer-based model before Dlinear.
- Autoformer [32]: it combines trend decomposition techniques with an auto-correlation mechanism, inspiring subsequent work such as FEDformer.
- Informer [37]: it proposes improvements to the Transformer model by utilizing a sparse self-attention mechanism and generative-style decoder, inspiring a series of subsequent Transformer-based LTSF models. This work was awarded Best Paper at AAAI 2021.

Classical RNN-based and CNN-based models, such as DeepAR [24] and LSTnet [15], have been demonstrated in previous works to be less effective than Transformer-based models in LTSF [37, 32]. Therefore, we did not include them in our baselines. We also noted other excellent works recently, such as MTS-Mixers [17], TimesNet [33], and Film [39]. However, due to limited resources, we could only select the LTSF models that were most relevant to our work and most representative at each stage as our baselines.

### A.1.3 Parameters

By default, PETformer uses 4 layers of Transformer encoder with a hidden dimension of 512, multi-head attention of 8, dropout rate of 0.5, and feedforward factor of 2. The default sub-sequence partitioning strategy uses a sub-sequence window length of 48 with a partitioning stride of 48. The default loss function is Smooth L1 Loss, with the FA mode in PET setting and the SA mode in MSI setting. The random seed is set as 2023.

However, different datasets may have distinct characteristics that require specific parameter adjustments. For instance, in tasks with higher noise, such as univariable prediction, we adopt the MAE loss function. Additionally, for datasets with a large number of variables, such as the Traffic dataset, we use the NCI mode in the MSI setting. We plan to release the code upon acceptance of the paper, and the full detailed parameter settings are available in our official open-source code.

### A.1.4 Environments

All experiments in this study are implemented in PyTorch and conducted on two NVIDIA V100 GPUs, each with 16GB of memory.

## A.2 Univariate forecasting

Table 7 presents the results of univariate time series forecasting for "oil temperature" in the ETT dataset. PETformer is observed to SOTA performance, surpassing all baseline models, including both Transformer-based and non-Transformer-based models. On average, PETformer demonstrates a 4.9% reduction in MSE and a 2.3% reduction in MAE compared to PatchTST. Compared to Dlinear, PETformer showcases a 15.4% improvement in MSE and an 7.2% improvement in MAE. This demonstrates that the PET and LSD designs effectively provide valuable prior knowledge for univariate time series forecasting tasks.

### A.3 Multi-channel separation

In this sub-section, we investigate why the MSI design can enhance predictive performance. We believe that channel-separation strategy can enlarge the number of training samples and thereby enhance the model’s ability to predict individual channels, leading to an overall improvement in the predictive ability across multiple channels.

Table 7: Univariate long-term series forecasting results. PETformer employs a look-back window length of  $l = 72$  for the ILI dataset and  $l = 720$  for the remaining datasets. It should be noted that other models typically perform optimally with different look-back window lengths. To avoid underestimating their performance, we conducted additional experiments with the other models using look-back window lengths of  $l \in \{24, 48, 72, 144\}$  for the ILI dataset and  $l \in \{96, 192, 336, 720\}$  for the other datasets, and the best result from these experiments was selected as their final outcome.

Models		PETformer (ours)		PatchTST (2023)		Dlinear (2023)		MICN (2023)		FEDformer* (2022)		Autoformer* (2021)		Informer* (2021)	
Metric		MSE	MAE	MSE	MAE	MSE	MAE	MSE	MAE	MSE	MAE	MSE	MAE	MSE	MAE
ETTh1	96	<b>0.052</b>	<b>0.174</b>	<u>0.055</u>	<u>0.179</u>	0.056	0.185	0.056	0.179	0.079	0.215	0.071	0.206	0.193	0.377
	192	<b>0.066</b>	<b>0.201</b>	<u>0.070</u>	<u>0.202</u>	0.077	0.218	0.071	0.203	0.104	0.245	0.114	0.262	0.217	0.395
	336	<b>0.075</b>	<b>0.217</b>	<u>0.077</u>	<u>0.225</u>	0.085	0.228	0.086	0.229	0.119	0.270	0.107	0.258	0.202	0.381
	720	<b>0.079</b>	<b>0.225</b>	<u>0.087</u>	<u>0.232</u>	0.159	0.322	0.150	0.316	0.142	0.299	0.126	0.283	0.183	0.355
ETTh2	96	<b>0.120</b>	0.272	0.127	0.273	0.122	<b>0.269</b>	0.128	0.271	0.128	0.271	0.153	0.306	0.213	0.373
	192	<b>0.156</b>	<b>0.316</b>	0.168	0.328	<u>0.166</u>	<u>0.320</u>	0.175	0.328	0.185	<u>0.330</u>	0.204	0.351	0.227	0.387
	336	<b>0.164</b>	<b>0.328</b>	0.172	0.338	0.188	<u>0.349</u>	0.192	0.354	0.231	0.378	0.246	0.389	0.242	0.401
	720	<b>0.208</b>	<b>0.367</b>	<u>0.223</u>	<u>0.382</u>	0.311	0.454	0.268	0.418	0.278	0.420	0.268	0.409	0.291	0.439
ETTm1	96	<b>0.026</b>	<b>0.120</b>	<u>0.026</u>	<u>0.121</u>	0.028	0.125	0.027	0.123	0.033	0.140	0.056	0.183	0.109	0.277
	192	<b>0.039</b>	<b>0.148</b>	<u>0.039</u>	<u>0.150</u>	0.045	0.156	0.043	0.154	0.058	0.186	0.081	0.216	0.151	0.310
	336	<b>0.052</b>	<b>0.171</b>	0.053	0.173	0.055	0.175	0.052	0.173	0.084	0.231	0.076	0.218	0.427	0.591
	720	<b>0.070</b>	<b>0.201</b>	<u>0.072</u>	<u>0.206</u>	0.076	0.209	0.075	<u>0.206</u>	0.102	0.250	0.110	0.267	0.438	0.586
ETTm2	96	0.062	0.181	0.063	0.186	<b>0.061</b>	<b>0.179</b>	0.063	0.183	0.067	0.198	0.065	0.189	0.088	0.225
	192	<b>0.087</b>	<b>0.222</b>	0.094	0.230	0.095	0.234	0.091	<u>0.225</u>	0.102	0.245	0.118	0.256	0.132	0.283
	336	<b>0.118</b>	<b>0.264</b>	<u>0.120</u>	<u>0.265</u>	0.122	0.265	0.121	<u>0.265</u>	0.130	0.279	0.154	0.305	0.180	0.336
	720	<b>0.163</b>	<b>0.317</b>	<u>0.171</u>	<u>0.321</u>	0.173	0.324	0.172	<u>0.317</u>	0.178	0.325	0.182	0.335	0.300	0.435
Avg.		<b>0.096</b>	<b>0.233</b>	<u>0.101</u>	<u>0.238</u>	0.114	0.251	0.111	0.247	0.126	0.268	0.133	0.277	0.225	0.384

\* denotes that the data originates from PatchTST [23], where the experimental reproduction strategy aligns consistently with this work.

Table 8: Results of PETformer on single-variable prediction under different modes. "Univariate" refers to the conventional univariate prediction task on the last dimension of the multivariate dataset. The remaining modes are trained in a multivariate prediction manner and then predict the last dimension of the multivariate dataset..

Models		Univariate		MSI/NCI		MSI/CI		MSI/SA		MSI/CA		DCM	
Metric		MSE	MAE	MSE	MAE	MSE	MAE	MSE	MAE	MSE	MAE	MSE	MAE
ETTh1	96	0.052	0.174	<u>0.051</u>	<b>0.170</b>	<b>0.050</b>	0.171	0.051	0.171	0.051	<u>0.170</u>	0.053	0.176
	192	<b>0.066</b>	0.201	<u>0.067</u>	<b>0.197</b>	0.067	0.198	0.068	0.199	0.068	<u>0.198</u>	0.070	0.203
	336	<b>0.075</b>	<b>0.217</b>	0.081	0.224	0.079	0.222	0.080	0.223	0.082	<u>0.225</u>	0.076	<u>0.218</u>
	720	<b>0.079</b>	<b>0.225</b>	0.092	0.238	<u>0.084</u>	<u>0.228</u>	0.093	0.240	0.094	0.240	0.115	0.266
Weather	96	0.0014	0.028	<u>0.0008</u>	0.020	0.0008	0.020	0.0008	0.020	<b>0.0008</b>	<b>0.019</b>	0.0012	0.025
	192	0.0013	0.026	0.0011	0.023	<u>0.0011</u>	<b>0.023</b>	0.0011	0.023	<b>0.0011</b>	<u>0.023</u>	0.0014	0.027
	336	0.0015	0.029	0.0013	0.026	<u>0.0013</u>	<u>0.026</u>	0.0013	0.026	<b>0.0013</b>	<b>0.026</b>	0.0018	0.031
	720	0.0020	0.034	0.0018	0.031	<u>0.0018</u>	<b>0.031</b>	0.0018	0.031	<b>0.0018</b>	<u>0.031</u>	0.0025	0.037
Electricity	96	0.213	0.312	0.185	0.293	<b>0.183</b>	<b>0.292</b>	0.185	0.292	0.187	0.292	0.680	0.642
	192	0.244	0.340	<u>0.218</u>	<u>0.318</u>	<b>0.215</b>	<b>0.317</b>	0.220	0.319	0.227	0.327	0.668	0.633
	336	0.293	0.389	0.254	0.348	<b>0.248</b>	<b>0.345</b>	0.250	0.347	0.258	0.357	0.663	0.631
	720	0.491	0.512	0.299	0.403	0.290	0.396	<u>0.280</u>	<u>0.388</u>	<b>0.265</b>	<b>0.372</b>	0.628	0.622
Traffic	96	0.118	0.195	<u>0.101</u>	0.166	0.101	<b>0.165</b>	<b>0.101</b>	0.166	0.108	0.178	0.582	0.580
	192	0.119	0.195	<b>0.106</b>	<b>0.170</b>	<u>0.106</u>	0.172	0.107	0.175	0.115	0.185	0.611	0.596
	336	0.120	0.198	0.106	0.174	<u>0.105</u>	<u>0.173</u>	<b>0.104</b>	<b>0.173</b>	0.114	0.189	0.627	0.606
	720	0.140	0.224	0.124	0.197	<u>0.122</u>	<u>0.194</u>	<b>0.119</b>	<b>0.191</b>	0.132	0.208	0.559	0.566
Avg.		0.126	0.206	0.106	0.187	<b>0.104</b>	<b>0.186</b>	<u>0.104</u>	<u>0.187</u>	0.107	0.190	0.334	0.366

Table 8 defines Univariate as the univariate prediction based solely on the last channel of the dataset. In contrast, MSI/NCI can be regarded as a pure univariate prediction task since it does not involve any inter-channel interaction. However, it significantly increases the number of training samples for univariate prediction tasks, as it utilizes data from all channels to perform univariate prediction. We can see that MSI/NCI exhibits a considerable improvement over Univariate, demonstrating that simply increasing the number of samples (even if they originate from other dimensions of the same dataset) can enhance the model's ability to predict a single channel. Note that the ETTh1, Weather, Electricity, and Traffic datasets contain 7, 21, 321, and 862 multivariate variables, respectively. Based on Table 8, we can observe that for the ETTh1 dataset, which contains only 7 variables, the MSI design even exhibits a decline in performance compared to Univariate. However, when the number of variables in the dataset increases significantly, resulting in a corresponding increase in the number of training samples, MSI/NCI can achieve a substantial improvement over Univariate.

MSI/CI represents a further strategy, which adds channel identifiers to each channel on the basis of MSI/NCI. Naturally, this further enhances the predictive ability on individual channels because it provides the model with identification information for different channels.

In addition, MSI/SA, MSI/CA, and DCM can be regarded as multivariate-predict-univariate tasks because they take into the interaction between channels. Here, MSI/SA and MSI/CA are both better than Univariate, which indicates the effectiveness of the MSI design. However, DCM performs relatively poorly, with much worse performance than Univariate. This fully demonstrates that the direct mixing of channels can seriously disrupt the temporal information within individual channels.

#### A.4 Varying look-back window

Table 9: The performance of PETformer on different look-back window lengths of  $l \in \{48, 96, 192, 336, 480, 720\}$ . The best results are highlighted in **bold**.

Input Length		48		96		192		336		480		720	
Metric		MSE	MAE	MSE	MAE	MSE	MAE	MSE	MAE	MSE	MAE	MSE	MAE
ETTh1	96	0.389	0.392	0.376	0.387	0.369	0.385	0.358	0.381	0.353	0.380	<b>0.347</b>	<b>0.377</b>
	192	0.443	0.424	0.429	0.417	0.414	0.410	0.397	0.404	<b>0.388</b>	<b>0.402</b>	0.390	0.404
	336	0.488	0.445	0.467	0.433	0.437	0.420	0.419	<b>0.417</b>	0.422	0.423	<b>0.419</b>	0.418
	720	0.482	0.462	0.471	0.459	0.449	0.450	0.443	0.453	0.438	<b>0.447</b>	<b>0.437</b>	0.449
ETTh2	96	0.299	0.340	0.288	0.339	0.284	0.338	0.281	0.333	<b>0.270</b>	<b>0.329</b>	0.272	0.329
	192	0.383	0.393	0.367	0.388	0.353	0.381	0.345	0.376	0.338	<b>0.374</b>	<b>0.338</b>	0.374
	336	0.397	0.410	0.369	0.398	0.349	0.394	0.336	0.380	0.330	<b>0.378</b>	<b>0.328</b>	0.380
	720	0.426	0.438	0.409	0.433	0.391	0.423	<b>0.385</b>	<b>0.422</b>	0.387	0.426	0.401	0.439
ETTm1	96	0.468	0.413	0.316	0.341	0.292	0.328	0.281	0.324	<b>0.279</b>	<b>0.323</b>	0.282	0.325
	192	0.514	0.437	0.366	0.367	0.333	0.353	0.321	0.351	0.320	0.349	<b>0.318</b>	<b>0.349</b>
	336	0.554	0.462	0.398	0.390	0.366	0.376	0.356	0.372	0.352	<b>0.370</b>	<b>0.348</b>	0.372
	720	0.601	0.489	0.463	0.427	0.425	0.412	0.416	0.407	0.415	0.407	<b>0.404</b>	<b>0.403</b>
ETTm2	96	0.190	0.271	0.174	0.255	0.167	0.248	0.160	<b>0.245</b>	0.163	0.248	<b>0.160</b>	0.248
	192	0.258	0.313	0.241	0.298	0.230	0.289	0.220	0.289	0.221	<b>0.288</b>	<b>0.217</b>	0.288
	336	0.324	0.353	0.298	0.335	0.283	0.327	0.271	0.320	<b>0.269</b>	<b>0.320</b>	0.274	0.326
	720	0.425	0.409	0.393	0.392	0.366	0.382	0.357	0.379	0.352	0.378	<b>0.345</b>	<b>0.376</b>
Electricity	96	0.222	0.292	0.171	0.254	0.138	0.229	0.131	0.223	0.128	0.221	<b>0.128</b>	<b>0.220</b>
	192	0.217	0.290	0.179	0.263	0.154	0.244	0.147	0.238	0.145	0.236	<b>0.144</b>	<b>0.236</b>
	336	0.235	0.307	0.195	0.279	0.177	0.268	0.163	0.255	0.161	0.253	<b>0.159</b>	<b>0.252</b>
	720	0.272	0.337	0.234	0.311	0.206	0.291	0.203	0.289	0.198	0.286	<b>0.195</b>	<b>0.286</b>
Traffic	96	0.671	0.379	0.465	0.299	0.396	0.260	0.373	0.249	0.365	0.245	<b>0.357</b>	<b>0.240</b>
	192	0.617	0.351	0.470	0.294	0.415	0.267	0.392	0.256	0.386	0.253	<b>0.376</b>	<b>0.248</b>
	336	0.640	0.362	0.486	0.301	0.430	0.274	0.403	0.261	0.396	0.258	<b>0.392</b>	<b>0.255</b>
	720	0.668	0.371	0.518	0.318	0.457	0.289	0.436	0.279	0.432	0.278	<b>0.430</b>	<b>0.276</b>
Weather	96	0.210	0.240	0.178	0.214	0.162	0.200	0.150	0.190	0.148	0.188	<b>0.146</b>	<b>0.186</b>
	192	0.245	0.269	0.225	0.254	0.205	0.240	0.194	0.232	0.192	0.229	<b>0.190</b>	<b>0.229</b>
	336	0.298	0.307	0.278	0.294	0.258	0.280	0.246	0.273	0.243	<b>0.271</b>	<b>0.241</b>	0.271
	720	0.372	0.355	0.352	0.344	0.333	0.333	0.320	0.326	0.315	0.324	<b>0.314</b>	<b>0.323</b>
Avg.		0.404	0.368	0.342	0.339	0.316	0.325	0.304	0.319	0.300	0.317	<b>0.298</b>	<b>0.317</b>

The length of the look-back window is a crucial factor in time series forecasting tasks, as it determines the amount of past data that the model can incorporate. Generally, a model that can effectively capture long-term temporal patterns is expected to exhibit better performance as the look-back window length increases. Therefore, we investigated the performance of PETformer under varying look-back window lengths, specifically  $l \in \{48, 96, 192, 336, 480, 720\}$ . The experimental results, as shown in Table 9, indicate that the performance of PETformer continuously improves as the look-back window length increases. This demonstrates PETformer’s ability to model long-term dependencies in time-series data effectively.

#### A.5 Baselines reproduction

PETformer exhibited more robust performance with an ultra-long look-back window (i.e.,  $l = 720$ ), while the baseline models showed significant performance variations across different look-back window lengths. To fairly evaluate the performance of PETformer and baseline models, we conducted additional experiments with the other models using look-back window lengths of  $l \in \{24, 48, 72, 144\}$  for the ILI dataset and  $l \in \{96, 192, 336, 720\}$  for the other datasets, and selected the best result from these experiments as their final outcome.

Table 10: Experimental results of PatchTST for multivariate time series forecasting with different look-back window lengths. To avoid underestimating its performance, additional experiments were conducted using look-back window lengths of  $l \in \{24, 48, 72, 144\}$  for the ILI dataset and  $l \in \{96, 192, 336, 720\}$  for the other datasets, and the best result from these experiments was selected as its final outcome. Note that we report the MAE corresponding to the best-performing MSE. ‘-’ indicates that we encountered issues while rerunning its official code. The best results are highlighted in **bold**.

Metric	Input Length		96(24)		192(48)		336(72)		720(144)		BestMSE	BestMAE	MAE with BestMSE
	MSE	MAE	MSE	MAE	MSE	MAE	MSE	MAE	MSE	MAE			
ETTh1	96	0.394	0.408	0.382	<b>0.401</b>	0.405	<b>0.376</b>	0.408	0.376	0.401	0.408	0.423	0.423
	192	0.446	0.434	0.428	0.425	<b>0.416</b>	<b>0.423</b>	0.416	0.416	0.423	0.423	0.440	0.440
	336	0.485	0.452	0.451	0.436	0.431	<b>0.435</b>	<b>0.425</b>	0.440	0.425	0.435	0.459	0.470
	720	0.480	0.471	0.452	<b>0.459</b>	0.449	0.466	<b>0.448</b>	0.470	0.448	0.459	0.470	0.470
ETTh2	96	0.294	0.343	0.285	0.340	0.275	<b>0.337</b>	<b>0.275</b>	0.338	0.275	0.337	0.338	0.338
	192	0.377	0.393	0.356	0.387	<b>0.338</b>	<b>0.378</b>	0.340	0.380	0.338	0.378	0.378	0.378
	336	0.382	0.410	0.351	0.396	<b>0.329</b>	<b>0.380</b>	0.330	0.384	0.329	0.380	0.380	0.380
	720	0.412	0.433	0.395	0.427	<b>0.379</b>	<b>0.422</b>	0.385	0.428	0.379	0.422	0.422	0.422
ETTm1	96	0.324	0.361	<b>0.293</b>	<b>0.342</b>	0.294	0.345	0.301	0.353	0.293	0.342	0.342	0.342
	192	0.363	0.384	<b>0.328</b>	<b>0.365</b>	0.333	0.371	0.334	0.374	0.328	0.365	0.365	0.365
	336	0.396	0.403	0.364	<b>0.388</b>	0.367	0.391	<b>0.362</b>	0.394	0.362	0.388	0.394	0.394
	720	0.454	0.437	0.422	0.423	<b>0.414</b>	<b>0.420</b>	0.421	0.422	0.414	0.420	0.420	0.420
ETTm2	96	0.176	0.258	0.169	0.254	0.165	<b>0.254</b>	<b>0.163</b>	0.255	0.163	0.254	0.255	0.255
	192	0.244	0.303	0.230	0.294	<b>0.221</b>	<b>0.292</b>	0.221	0.297	0.221	0.292	0.292	0.292
	336	0.302	0.342	0.281	0.329	0.279	<b>0.329</b>	<b>0.270</b>	0.329	0.270	0.329	0.329	0.329
	720	0.399	0.396	0.373	0.384	0.365	0.383	<b>0.347</b>	<b>0.378</b>	0.347	0.378	0.378	0.378
Electricity	96	0.171	0.256	0.136	0.228	<b>0.130</b>	<b>0.223</b>	0.140	0.239	0.130	0.223	0.223	0.223
	192	0.178	0.264	0.152	0.243	<b>0.147</b>	<b>0.240</b>	0.155	0.255	0.147	0.240	0.240	0.240
	336	0.194	0.280	0.168	0.261	<b>0.164</b>	<b>0.257</b>	0.172	0.271	0.164	0.257	0.257	0.257
	720	0.234	0.313	0.206	0.294	<b>0.203</b>	<b>0.292</b>	0.210	0.301	0.203	0.292	0.292	0.292
ILI	24	-	-	1.475	0.742	<b>1.356</b>	<b>0.732</b>	1.591	0.870	1.356	0.732	0.732	0.732
	36	-	-	<b>1.244</b>	<b>0.705</b>	1.397	0.770	1.512	0.852	1.244	0.705	0.705	0.705
	48	-	-	<b>1.604</b>	<b>0.791</b>	1.836	0.902	1.658	0.863	1.604	0.791	0.791	0.791
	60	-	-	1.649	0.863	<b>1.648</b>	<b>0.860</b>	1.990	0.960	1.648	0.860	0.860	0.860
Traffic	96	0.460	0.292	0.386	0.258	0.373	0.254	<b>0.367</b>	<b>0.253</b>	0.367	0.253	0.253	0.253
	192	0.466	0.292	0.404	0.264	0.390	0.261	<b>0.382</b>	<b>0.259</b>	0.382	0.259	0.259	0.259
	336	0.480	0.299	0.418	0.272	0.403	0.268	<b>0.396</b>	<b>0.267</b>	0.396	0.267	0.267	0.267
	720	0.514	0.317	0.448	0.290	0.433	<b>0.285</b>	<b>0.433</b>	0.287	0.433	0.285	0.287	0.287
Weather	96	0.181	0.221	0.160	0.205	0.156	0.205	<b>0.147</b>	<b>0.198</b>	0.147	0.198	0.198	0.198
	192	0.225	0.259	0.204	0.245	0.196	0.242	<b>0.190</b>	<b>0.241</b>	0.190	0.241	0.241	0.241
	336	0.278	0.297	0.258	0.285	0.249	<b>0.283</b>	<b>0.243</b>	0.284	0.243	0.283	0.284	0.284
	720	0.351	0.346	0.329	0.337	0.319	0.334	<b>0.305</b>	<b>0.328</b>	0.305	0.328	0.328	0.328

We performed these experiments on their publicly available official repositories, prioritizing their default parameters and only modifying the look-back window length  $l$  and the prediction horizon  $h$ . The official open-source codes for these baseline models are as follows:

- PatchTST: <https://github.com/yuqinie98/patchtst>
- Dlinear: <https://github.com/cure-lab/LTSF-Linear>
- Micn: <https://github.com/wanghq21/MICN>
- Crossformer: <https://github.com/Thinklab-SJTU/Crossformer>
- FEDformer: <https://github.com/MAZiqing/FEDformer>
- Autoformer: <https://github.com/thuml/Autoformer>
- Informer: <https://github.com/zhouhaoyi/Informer2020>

The results of our experiment reproduction are presented in Table 10, 11, 12, 13, 14, 15, and 16. It should be noted that reproducing these experiments requires a significant amount of computational resources. To save computational resources, the data for FEDformer, Autoformer, and Informer were directly sourced from PatchTST [23] since its reproduction strategy is consistent with our work.

## A.6 Robustness analysis

To ensure the robustness of our experimental findings, we conducted each experiment three times using different random seeds: 2023, 2024, and 2025. The mean and standard deviation of the results are summarized in Table 17, which shows that the variances are notably small. This indicates that our model is robust to the choice of random seeds, and the reported results can be considered reliable.

Table 11: Experimental results of PatchTST for univariate time series forecasting with different look-back window lengths. To avoid underestimating its performance, additional experiments were conducted using look-back window lengths of  $l \in \{24, 48, 72, 144\}$  for the ILI dataset and  $l \in \{96, 192, 336, 720\}$  for the other datasets, and the best result from these experiments was selected as its final outcome. Note that we report the MAE corresponding to the best-performing MSE. The best results are highlighted in **bold**.

Input Length	96				192				336				720				BestMSE	BestMAE	MAE with BestMSE
	Metric	MSE	MAE	MSE	MAE	MSE	MAE	MSE	MAE	MSE	MAE	MSE	MAE	MSE	MAE	MSE			
ETTh1	96	0.057	0.180	0.056	0.179	<b>0.055</b>	<b>0.179</b>	0.059	0.192	0.055	0.179	0.055	0.179	0.055	0.179	0.055	0.179	0.055	0.179
	192	0.075	0.209	<b>0.070</b>	<b>0.202</b>	0.071	0.205	0.072	0.216	0.070	0.202	0.070	0.202	0.070	0.202	0.070	0.202	0.070	0.202
	336	0.092	0.238	0.083	0.227	0.082	0.226	<b>0.077</b>	<b>0.225</b>	0.077	0.225	0.077	0.225	0.077	0.225	0.077	0.225	0.077	0.225
	720	0.097	0.245	0.091	0.237	<b>0.087</b>	<b>0.232</b>	0.093	0.245	0.087	0.232	0.087	0.232	0.087	0.232	0.087	0.232	0.087	0.232
ETTh2	96	<b>0.127</b>	<b>0.273</b>	0.131	0.280	0.129	0.282	0.138	0.291	0.127	0.273	0.127	0.273	0.127	0.273	0.127	0.273	0.127	0.273
	192	0.178	<b>0.328</b>	0.180	0.334	<b>0.168</b>	0.328	0.172	0.332	0.168	0.328	0.168	0.328	0.168	0.328	0.168	0.328	0.168	0.328
	336	0.221	0.374	0.199	0.360	0.185	0.351	<b>0.172</b>	<b>0.338</b>	0.172	0.338	0.172	0.338	0.172	0.338	0.172	0.338	0.172	0.338
	720	0.250	0.403	0.234	0.392	<b>0.223</b>	<b>0.382</b>	0.233	0.388	0.223	0.382	0.223	0.382	0.223	0.382	0.223	0.382	0.223	0.382
ETTm1	96	0.029	0.126	0.028	0.126	<b>0.026</b>	<b>0.121</b>	0.027	0.123	0.026	0.121	0.026	0.121	0.026	0.121	0.026	0.121	0.026	0.121
	192	0.044	0.158	0.041	0.153	<b>0.039</b>	<b>0.150</b>	0.041	0.152	0.039	0.150	0.039	0.150	0.039	0.150	0.039	0.150	0.039	0.150
	336	0.057	0.184	0.054	0.177	<b>0.053</b>	<b>0.173</b>	0.054	0.176	0.053	0.173	0.053	0.173	0.053	0.173	0.053	0.173	0.053	0.173
	720	0.081	0.218	0.077	0.211	0.075	0.207	<b>0.072</b>	<b>0.206</b>	0.072	0.206	0.072	0.206	0.072	0.206	0.072	0.206	0.072	0.206
ETTm2	96	0.064	<b>0.181</b>	0.066	0.188	0.065	0.187	<b>0.063</b>	0.186	0.063	0.181	0.063	0.181	0.063	0.181	0.063	0.181	0.063	0.181
	192	0.097	0.231	0.099	0.235	<b>0.094</b>	<b>0.230</b>	0.094	0.235	0.094	0.230	0.094	0.230	0.094	0.230	0.094	0.230	0.094	0.230
	336	0.129	0.270	0.127	0.271	<b>0.120</b>	<b>0.265</b>	0.124	0.272	0.120	0.265	0.120	0.265	0.120	0.265	0.120	0.265	0.120	0.265
	720	0.181	0.330	0.179	0.331	<b>0.171</b>	<b>0.321</b>	0.173	0.326	0.171	0.321	0.171	0.321	0.171	0.321	0.171	0.321	0.171	0.321

Both the main text and the appendix present results obtained using a fixed random seed of 2023, and these results are consistent with the results obtained using the other random seeds.

## A.7 Forecast showcases

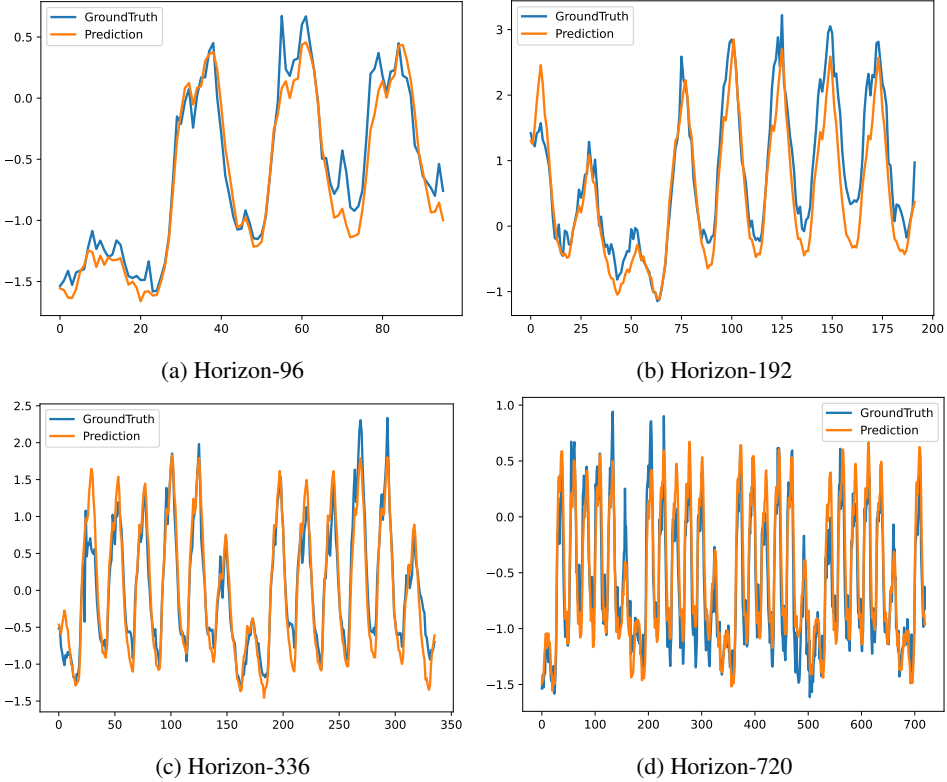


Figure 5: Prediction cases for the Electricity dataset with a look-back window length of  $l = 720$  and a forecast horizon of  $h \in \{96, 192, 336, 720\}$ .

Table 12: Experimental results of Dlinear for multivariate time series forecasting with different look-back window lengths. To avoid underestimating its performance, additional experiments were conducted using look-back window lengths of  $l \in \{24, 48, 72, 144\}$  for the ILI dataset and  $l \in \{96, 192, 336, 720\}$  for the other datasets, and the best result from these experiments was selected as its final outcome. Note that we report the MAE corresponding to the best-performing MSE. The best results are highlighted in **bold**.

Input Length	96(24)				192(48)				336(72)				720(144)				BestMSE	BestMAE	MAE with BestMSE
	Metric	MSE	MAE	MSE	MAE	MSE	MAE	MSE	MAE	MSE	MAE	MSE	MSE	MAE	MSE	MAE			
ETTh1	96	0.383	<b>0.396</b>	0.383	0.399	0.384	0.405	<b>0.378</b>	0.402	0.378	0.396	0.396	0.402						
	192	0.433	0.426	0.422	<b>0.421</b>	0.443	0.450	<b>0.415</b>	0.425	0.415	0.421	0.421	0.425						
	336	0.491	0.467	0.480	0.466	<b>0.447</b>	<b>0.448</b>	0.449	0.448	0.447	0.448	0.448	0.448						
	720	0.527	0.518	<b>0.480</b>	<b>0.489</b>	0.503	0.514	0.506	0.516	0.480	0.489	0.489	0.489						
ETTh2	96	0.330	0.386	0.301	0.357	<b>0.282</b>	<b>0.346</b>	0.293	0.360	0.282	0.346	0.346	0.346						
	192	0.449	0.454	0.399	0.426	<b>0.350</b>	<b>0.396</b>	0.415	0.440	0.350	0.396	0.396	0.396						
	336	0.463	0.467	0.457	0.471	<b>0.410</b>	<b>0.437</b>	0.453	0.459	0.410	0.437	0.437	0.437						
	720	0.714	0.605	0.678	0.589	<b>0.587</b>	<b>0.544</b>	0.793	0.630	0.587	0.544	0.544	0.544						
ETTm1	96	0.343	0.371	<b>0.366</b>	<b>0.345</b>	0.312	0.355	0.307	0.351	0.306	0.345	0.345	0.345						
	192	0.381	0.390	0.342	0.368	<b>0.335</b>	<b>0.365</b>	0.345	0.379	0.335	0.365	0.365	0.365						
	336	0.418	0.421	0.379	0.392	<b>0.373</b>	<b>0.391</b>	0.403	0.431	0.373	0.391	0.391	0.391						
	720	0.475	0.454	0.461	0.457	0.425	<b>0.421</b>	<b>0.422</b>	0.422	0.422	0.421	0.421	0.422						
ETTm2	96	0.193	0.288	0.191	0.286	0.172	0.265	<b>0.164</b>	<b>0.259</b>	0.164	0.259	0.259	0.259						
	192	0.284	0.352	0.253	0.323	<b>0.233</b>	0.314	0.234	<b>0.312</b>	0.233	0.312	0.312	0.314						
	336	0.344	0.395	0.306	0.365	0.295	0.359	<b>0.291</b>	<b>0.355</b>	0.291	0.355	0.355	0.355						
	720	0.438	0.444	0.451	0.458	0.426	0.439	<b>0.407</b>	<b>0.433</b>	0.407	0.433	0.433	0.433						
Electricity	96	0.194	0.277	0.152	0.246	0.140	0.237	<b>0.133</b>	<b>0.230</b>	0.133	0.230	0.230	0.230						
	192	0.193	0.280	0.163	0.258	0.153	0.250	<b>0.147</b>	<b>0.244</b>	0.147	0.244	0.244	0.244						
	336	0.206	0.296	0.178	0.275	0.168	0.267	<b>0.162</b>	<b>0.261</b>	0.162	0.261	0.261	0.261						
	720	0.242	0.328	0.213	0.308	0.203	0.300	<b>0.196</b>	<b>0.294</b>	0.196	0.294	0.294	0.294						
ILI	24	4.127	1.408	2.272	1.010	2.337	1.081	<b>2.000</b>	<b>0.987</b>	2.000	0.987	0.987	0.987						
	36	3.983	1.359	2.343	<b>1.008</b>	2.430	1.056	<b>2.202</b>	1.026	2.202	1.008	1.026	1.026						
	48	3.650	1.299	2.744	1.126	2.411	1.088	<b>2.278</b>	<b>1.059</b>	2.278	1.059	1.059	1.059						
	60	3.897	1.365	2.627	1.112	<b>2.478</b>	<b>1.111</b>	2.482	1.119	2.478	1.111	1.111	1.111						
Traffic	96	0.651	0.397	0.451	0.302	0.411	0.282	<b>0.385</b>	<b>0.269</b>	0.385	0.269	0.269	0.269						
	192	0.598	0.370	0.458	0.304	0.422	0.287	<b>0.395</b>	<b>0.273</b>	0.395	0.273	0.273	0.273						
	336	0.605	0.373	0.472	0.313	0.435	0.295	<b>0.409</b>	<b>0.281</b>	0.409	0.281	0.281	0.281						
	720	0.645	0.395	0.503	0.333	0.466	0.315	<b>0.449</b>	<b>0.305</b>	0.449	0.305	0.305	0.305						
Weather	96	0.202	0.269	0.184	0.243	0.178	0.244	<b>0.169</b>	<b>0.231</b>	0.169	0.231	0.231	0.231						
	192	0.236	0.292	0.224	0.281	0.216	0.274	<b>0.213</b>	<b>0.273</b>	0.213	0.273	0.273	0.273						
	336	0.288	0.339	0.270	0.319	0.264	0.316	<b>0.260</b>	<b>0.314</b>	0.260	0.314	0.314	0.314						
	720	0.353	0.394	0.348	0.389	0.323	0.362	<b>0.315</b>	<b>0.353</b>	0.315	0.353	0.353	0.353						

In this sub-section, we present the prediction showcases of PETformer on the large datasets, as shown in Figure 5 and Figure 6. These results demonstrate that PETformer can correctly learn the inherent trends and periodicity of time series data, thus accurately predicting the future trends of the data.

Table 13: Experimental results of Dlinear for univariate time series forecasting with different look-back window lengths. To avoid underestimating its performance, additional experiments were conducted using look-back window lengths of  $l \in \{24, 48, 72, 144\}$  for the ILI dataset and  $l \in \{96, 192, 336, 720\}$  for the other datasets, and the best result from these experiments was selected as its final outcome. Note that we report the MAE corresponding to the best-performing MSE. The best results are highlighted in **bold**.

Input Length		96		192		336		720		BestMSE	BestMAE	MAE with BestMSE
Metric		MSE	MAE	MSE	MAE	MSE	MAE	MSE	MAE			
ETTh1	96	0.060	0.181	0.058	0.179	<b>0.056</b>	<b>0.179</b>	0.066	0.195	0.056	0.179	0.179
	192	0.083	0.214	<b>0.071</b>	<b>0.203</b>	0.075	0.208	0.096	0.240	0.071	0.203	0.203
	336	0.104	0.250	<b>0.086</b>	<b>0.229</b>	0.091	0.237	0.112	0.264	0.086	0.229	0.229
	720	<b>0.150</b>	<b>0.316</b>	0.170	0.338	0.168	0.335	0.206	0.376	0.150	0.316	0.316
ETTh2	96	<b>0.128</b>	<b>0.271</b>	0.133	0.278	0.131	0.279	0.143	0.295	0.128	0.271	0.271
	192	0.182	<b>0.327</b>	0.178	0.329	<b>0.175</b>	0.328	0.181	0.338	0.175	0.327	0.328
	336	0.231	0.378	0.217	0.372	0.211	0.368	<b>0.192</b>	<b>0.354</b>	0.192	0.354	0.354
	720	0.317	0.460	0.303	0.449	0.294	0.440	<b>0.268</b>	<b>0.418</b>	0.268	0.418	0.418
ETTm1	96	0.032	0.132	0.029	0.126	<b>0.027</b>	<b>0.123</b>	0.027	0.124	0.027	0.123	0.123
	192	0.051	0.167	0.049	0.164	0.050	0.167	<b>0.043</b>	<b>0.154</b>	0.043	0.154	0.154
	336	0.086	0.222	0.065	0.188	0.069	0.195	<b>0.052</b>	<b>0.173</b>	0.052	0.173	0.173
	720	0.098	0.234	0.091	0.226	0.082	0.213	<b>0.075</b>	<b>0.206</b>	0.075	0.206	0.206
ETTm2	96	0.070	0.191	0.067	0.187	<b>0.063</b>	<b>0.183</b>	0.063	0.184	0.063	0.183	0.183
	192	0.103	0.237	0.094	0.228	<b>0.091</b>	<b>0.225</b>	0.094	0.230	0.091	0.225	0.225
	336	0.135	0.278	0.123	0.266	0.129	0.273	<b>0.121</b>	<b>0.265</b>	0.121	0.265	0.265
	720	0.188	0.332	0.176	0.322	<b>0.172</b>	<b>0.317</b>	0.176	0.325	0.172	0.317	0.317

Table 14: Experimental results of MICN for multivariate time series forecasting with different look-back window lengths. To avoid underestimating its performance, additional experiments were conducted using look-back window lengths of  $l \in \{24, 48, 72, 144\}$  for the ILI dataset and  $l \in \{96, 192, 336, 720\}$  for the other datasets, and the best result from these experiments was selected as its final outcome. Note that we report the MAE corresponding to the best-performing MSE. The best results are highlighted in **bold**.

Input Length		96(24)		192(48)		336(72)		720(144)		BestMSE	BestMAE	MAE with BestMSE
Metric		MSE	MAE	MSE	MAE	MSE	MAE	MSE	MAE			
ETTh1	96	0.404	0.431	0.421	0.435	<b>0.404</b>	<b>0.429</b>	0.412	0.444	0.404	0.429	0.429
	192	0.504	0.492	0.485	<b>0.483</b>	0.511	0.506	<b>0.475</b>	0.484	0.475	0.483	0.484
	336	0.545	0.530	0.662	0.609	<b>0.482</b>	<b>0.489</b>	0.652	0.589	0.482	0.489	0.489
	720	0.830	0.706	<b>0.599</b>	<b>0.576</b>	0.697	0.631	0.871	0.713	0.599	0.576	0.576
ETTh2	96	<b>0.289</b>	<b>0.354</b>	0.322	0.383	0.290	0.356	0.318	0.386	0.289	0.354	0.354
	192	0.441	0.454	0.431	0.446	0.415	<b>0.441</b>	<b>0.408</b>	0.444	0.408	0.441	0.444
	336	<b>0.547</b>	<b>0.516</b>	0.768	0.628	0.627	0.573	0.985	0.724	0.547	0.516	0.516
	720	<b>0.834</b>	<b>0.688</b>	1.135	0.787	1.340	0.858	1.063	0.765	0.834	0.688	0.688
ETTm1	96	0.313	0.363	<b>0.301</b>	<b>0.352</b>	0.305	0.354	0.308	0.358	0.301	0.352	0.352
	192	0.361	0.388	<b>0.344</b>	<b>0.380</b>	0.362	0.399	0.363	0.396	0.344	0.380	0.380
	336	0.385	0.415	<b>0.379</b>	<b>0.401</b>	0.382	0.405	0.446	0.457	0.379	0.401	0.401
	720	0.445	0.454	0.438	0.450	0.441	<b>0.429</b>	<b>0.429</b>	0.429	0.429	0.429	0.429
ETTm2	96	0.178	<b>0.272</b>	<b>0.177</b>	0.274	0.189	0.287	0.183	0.283	0.177	0.272	0.274
	192	<b>0.236</b>	<b>0.310</b>	0.310	0.376	0.239	0.323	0.245	0.326	0.236	0.310	0.310
	336	<b>0.299</b>	<b>0.350</b>	0.367	0.421	0.348	0.385	0.305	0.366	0.299	0.350	0.350
	720	0.430	0.449	0.477	0.477	<b>0.421</b>	<b>0.434</b>	0.445	0.455	0.421	0.434	0.434
Electricity	96	0.169	0.275	0.156	0.263	0.162	0.272	<b>0.151</b>	<b>0.260</b>	0.151	0.260	0.260
	192	0.179	0.287	0.174	0.285	0.176	0.285	<b>0.165</b>	<b>0.276</b>	0.165	0.276	0.276
	336	<b>0.183</b>	<b>0.291</b>	0.191	0.301	0.194	0.301	0.236	0.335	0.183	0.291	0.291
	720	0.212	0.319	0.218	0.325	0.222	0.327	<b>0.201</b>	<b>0.312</b>	0.201	0.312	0.312
ILI	24	3.614	1.283	<b>2.483</b>	<b>1.058</b>	2.559	1.099	2.627	1.120	2.483	1.058	1.058
	36	2.929	1.099	<b>2.370</b>	<b>0.987</b>	2.483	1.023	2.520	1.035	2.370	0.987	0.987
	48	2.593	1.033	2.384	1.009	<b>2.371</b>	<b>1.007</b>	2.674	1.056	2.371	1.007	1.007
	60	2.726	1.090	<b>2.513</b>	<b>1.055</b>	2.694	1.112	2.772	1.100	2.513	1.055	1.055
Traffic	96	0.515	0.308	0.488	0.300	0.461	<b>0.290</b>	<b>0.445</b>	0.295	0.445	0.290	0.295
	192	0.536	0.314	0.494	<b>0.301</b>	0.482	0.302	<b>0.461</b>	0.302	0.461	0.301	0.302
	336	0.537	0.313	0.526	0.304	0.487	<b>0.300</b>	<b>0.483</b>	0.307	0.483	0.300	0.307
	720	0.603	0.328	0.541	0.318	<b>0.527</b>	<b>0.310</b>	0.531	0.325	0.527	0.310	0.310
Weather	96	<b>0.167</b>	<b>0.231</b>	0.178	0.249	0.170	0.235	0.172	0.237	0.167	0.231	0.231
	192	0.224	0.287	0.223	0.293	0.214	0.277	<b>0.212</b>	<b>0.271</b>	0.212	0.271	0.271
	336	<b>0.275</b>	0.337	0.286	0.349	0.278	<b>0.326</b>	0.275	0.330	0.275	0.326	0.337
	720	0.334	0.378	<b>0.312</b>	<b>0.349</b>	0.318	0.363	0.326	0.357	0.312	0.349	0.349

Table 15: Experimental results of MICN for univariate time series forecasting with different look-back window lengths. To avoid underestimating its performance, additional experiments were conducted using look-back window lengths of  $l \in \{24, 48, 72, 144\}$  for the ILI dataset and  $l \in \{96, 192, 336, 720\}$  for the other datasets, and the best result from these experiments was selected as its final outcome. Note that we report the MAE corresponding to the best-performing MSE. The best results are highlighted in **bold**.

Input Length		96		192		336		720		BestMSE	BestMAE	MAE with BestMSE
Metric		MSE	MAE	MSE	MAE	MSE	MAE	MSE	MAE			
ETTh1	96	0.058	<b>0.183</b>	<b>0.056</b>	0.185	0.059	0.190	0.095	0.240	0.056	0.183	0.185
	192	0.088	0.221	<b>0.077</b>	<b>0.218</b>	0.087	0.235	0.135	0.294	0.077	0.218	0.218
	336	<b>0.085</b>	<b>0.228</b>	0.092	0.240	0.089	0.237	0.102	0.251	0.085	0.228	0.228
	720	0.159	0.326	<b>0.159</b>	<b>0.322</b>	0.176	0.343	0.210	0.380	0.159	0.322	0.322
ETTh2	96	0.142	0.285	<b>0.122</b>	<b>0.269</b>	0.127	0.276	0.135	0.290	0.122	0.269	0.269
	192	0.211	0.353	0.169	0.324	<b>0.166</b>	<b>0.320</b>	0.251	0.406	0.166	0.320	0.320
	336	0.250	0.390	0.191	0.349	<b>0.188</b>	<b>0.349</b>	0.227	0.387	0.188	0.349	0.349
	720	0.328	0.470	0.348	0.485	<b>0.311</b>	<b>0.454</b>	0.359	0.490	0.311	0.454	0.454
ETTm1	96	0.034	0.141	0.030	0.134	0.030	0.131	<b>0.028</b>	<b>0.125</b>	0.028	0.125	0.125
	192	0.055	0.174	0.049	0.164	<b>0.045</b>	<b>0.156</b>	0.046	0.165	0.045	0.156	0.156
	336	0.076	0.205	0.072	0.197	<b>0.055</b>	<b>0.175</b>	0.057	0.184	0.055	0.175	0.175
	720	0.087	0.222	0.083	0.217	0.078	0.210	<b>0.076</b>	<b>0.209</b>	0.076	0.209	0.209
ETTm2	96	0.063	0.182	<b>0.061</b>	<b>0.179</b>	0.064	0.184	0.069	0.196	0.061	0.179	0.179
	192	0.117	0.257	0.100	0.238	0.095	<b>0.232</b>	<b>0.095</b>	0.234	0.095	0.232	0.234
	336	0.139	0.283	0.130	0.275	<b>0.122</b>	<b>0.265</b>	0.130	0.277	0.122	0.265	0.265
	720	0.188	0.332	0.181	0.326	0.202	0.348	<b>0.173</b>	<b>0.324</b>	0.173	0.324	0.324

Table 16: Experimental results of Crossformer for multivariate time series forecasting with different look-back window lengths. To avoid underestimating its performance, additional experiments were conducted using look-back window lengths of  $l \in \{24, 48, 72, 144\}$  for the ILI dataset and  $l \in \{96, 192, 336, 720\}$  for the other datasets, and the best result from these experiments was selected as its final outcome. Note that we report the MAE corresponding to the best-performing MSE. The best results are highlighted in **bold**.

Input Length		96(24)		192(48)		336(72)		720(144)		BestMSE	BestMAE	MAE with BestMSE
Metric		MSE	MAE	MSE	MAE	MSE	MAE	MSE	MAE			
ETTh1	96	0.409	0.432	0.402	0.424	0.394	<b>0.418</b>	<b>0.380</b>	0.419	0.380	0.418	0.419
	192	0.458	0.459	0.448	0.447	0.423	<b>0.436</b>	<b>0.419</b>	0.445	0.419	0.436	0.445
	336	0.509	0.492	0.470	0.464	<b>0.438</b>	<b>0.451</b>	0.471	0.483	0.438	0.451	0.451
	720	0.696	0.632	0.516	0.518	<b>0.508</b>	<b>0.514</b>	0.524	0.527	0.508	0.514	0.514
ETTh2	96	0.402	0.425	0.398	0.419	0.395	<b>0.417</b>	<b>0.383</b>	0.420	0.383	0.417	0.420
	192	0.452	0.456	0.439	0.444	0.427	<b>0.438</b>	<b>0.421</b>	0.450	0.421	0.438	0.450
	336	0.533	0.506	0.482	0.468	<b>0.449</b>	<b>0.459</b>	0.455	0.469	0.449	0.459	0.459
	720	0.577	0.557	0.781	0.668	0.501	0.509	<b>0.472</b>	<b>0.497</b>	0.472	0.497	0.497
ETTm1	96	0.355	0.391	0.314	0.366	0.302	0.359	<b>0.295</b>	<b>0.350</b>	0.295	0.350	0.350
	192	0.416	0.433	0.379	0.412	0.341	0.387	<b>0.339</b>	<b>0.381</b>	0.339	0.381	0.381
	336	0.486	0.479	0.447	0.462	<b>0.419</b>	<b>0.432</b>	0.419	0.432	0.419	0.432	0.432
	720	0.624	0.570	<b>0.579</b>	<b>0.551</b>	0.637	0.577	0.728	0.620	0.579	0.551	0.551
ETTm2	96	0.356	0.388	0.323	0.372	0.305	0.361	<b>0.296</b>	<b>0.352</b>	0.296	0.352	0.352
	192	0.422	0.440	0.381	0.412	0.355	0.391	<b>0.342</b>	<b>0.385</b>	0.342	0.385	0.385
	336	0.507	0.494	0.430	0.447	0.420	0.431	<b>0.410</b>	<b>0.425</b>	0.410	0.425	0.425
	720	0.598	0.552	<b>0.563</b>	<b>0.538</b>	0.592	0.548	0.697	0.617	0.563	0.538	0.538
Electricity	96	0.224	0.310	0.207	0.296	<b>0.198</b>	<b>0.292</b>	0.222	0.303	0.198	0.292	0.292
	192	0.281	0.345	0.289	0.349	<b>0.266</b>	<b>0.330</b>	0.294	0.348	0.266	0.330	0.330
	336	0.351	0.394	<b>0.343</b>	<b>0.377</b>	0.353	0.384	0.359	0.392	0.343	0.377	0.377
	720	0.426	0.439	0.431	0.440	0.400	<b>0.416</b>	<b>0.398</b>	0.422	0.398	0.416	0.422
ILI	24	4.721	1.524	<b>3.217</b>	<b>1.198</b>	3.383	1.249	3.444	1.275	3.217	1.198	1.198
	36	4.148	1.379	3.144	1.162	3.151	<b>1.157</b>	<b>3.136</b>	1.199	3.136	1.157	1.199
	48	4.023	1.354	3.524	1.266	3.386	<b>1.186</b>	<b>3.331</b>	1.236	3.331	1.186	1.236
	60	4.114	1.369	3.843	1.324	3.658	1.268	<b>3.609</b>	<b>1.265</b>	3.609	1.265	1.265
Traffic	96	0.512	0.288	0.501	0.281	0.489	0.276	<b>0.487</b>	<b>0.274</b>	0.487	0.274	0.274
	192	0.538	0.297	0.516	0.286	0.503	0.281	<b>0.497</b>	<b>0.279</b>	0.497	0.279	0.279
	336	0.569	0.315	0.532	0.291	0.528	0.292	<b>0.517</b>	<b>0.285</b>	0.517	0.285	0.285
	720	0.613	0.336	0.603	0.333	0.593	0.326	<b>0.584</b>	<b>0.323</b>	0.584	0.323	0.323
Weather	96	0.162	0.231	0.149	0.217	0.147	0.211	<b>0.144</b>	<b>0.208</b>	0.144	0.208	0.208
	192	0.211	0.281	0.204	0.277	0.194	<b>0.261</b>	<b>0.192</b>	0.263	0.192	0.261	0.263
	336	0.270	0.328	0.250	0.312	<b>0.246</b>	<b>0.306</b>	0.251	0.312	0.246	0.306	0.306
	720	0.352	0.382	0.340	0.375	0.322	0.363	<b>0.318</b>	<b>0.361</b>	0.318	0.361	0.361

Table 17: Quantitative results of PETformer with fluctuations across different random seeds: 2023, 2024, and 2025.

Random seed		2023		2024		2025		Standard deviation	
Metric		MSE	MAE	MSE	MAE	MSE	MAE	MSE	MAE
ETTh1	96	0.347	0.377	0.348	0.379	0.350	0.379	0.348±0.0014	0.378±0.0010
	192	0.390	0.404	0.388	0.402	0.392	0.407	0.390±0.0020	0.404±0.0021
	336	0.419	0.418	0.418	0.421	0.414	0.416	0.417±0.0028	0.419±0.0027
	720	0.437	0.449	0.474	0.473	0.436	0.448	0.449±0.0216	0.457±0.0139
ETTh2	96	0.272	0.329	0.270	0.329	0.272	0.330	0.271±0.0011	0.329±0.0006
	192	0.338	0.374	0.338	0.375	0.334	0.372	0.336±0.0019	0.374±0.0014
	336	0.328	0.380	0.326	0.379	0.331	0.384	0.328±0.0025	0.381±0.0026
	720	0.401	0.439	0.399	0.437	0.398	0.436	0.399±0.0016	0.437±0.0019
ETTm1	96	0.282	0.325	0.281	0.324	0.277	0.324	0.280±0.0023	0.324±0.0007
	192	0.318	0.349	0.317	0.349	0.318	0.349	0.318±0.0007	0.349±0.0005
	336	0.348	0.372	0.347	0.370	0.349	0.370	0.348±0.0010	0.371±0.0009
	720	0.404	0.403	0.405	0.402	0.405	0.402	0.405±0.0005	0.402±0.0001
ETTm2	96	0.160	0.248	0.161	0.246	0.159	0.246	0.160±0.0007	0.247±0.0008
	192	0.217	0.288	0.219	0.290	0.218	0.287	0.218±0.0009	0.288±0.0016
	336	0.274	0.326	0.279	0.328	0.276	0.326	0.276±0.0024	0.327±0.0015
	720	0.345	0.376	0.345	0.377	0.352	0.380	0.348±0.0041	0.378±0.0022
Electricity	96	0.128	0.220	0.128	0.220	0.128	0.220	0.128±0.0002	0.220±0.0002
	192	0.144	0.236	0.144	0.236	0.144	0.236	0.144±0.0002	0.236±0.0002
	336	0.159	0.252	0.158	0.252	0.158	0.251	0.159±0.0004	0.252±0.0006
	720	0.195	0.286	0.193	0.284	0.194	0.284	0.194±0.0008	0.285±0.0010
Traffic	96	0.357	0.240	0.359	0.241	0.359	0.241	0.358±0.0010	0.241±0.0005
	192	0.376	0.248	0.377	0.249	0.376	0.248	0.376±0.0006	0.249±0.0003
	336	0.392	0.255	0.391	0.255	0.391	0.255	0.391±0.0004	0.255±0.0002
	720	0.430	0.276	0.431	0.277	0.429	0.276	0.430±0.0006	0.276±0.0004
Weather	96	0.146	0.186	0.145	0.184	0.146	0.184	0.145±0.0002	0.185±0.0009
	192	0.190	0.229	0.189	0.228	0.190	0.228	0.190±0.0007	0.228±0.0005
	336	0.241	0.271	0.243	0.272	0.242	0.271	0.242±0.0009	0.271±0.0005
	720	0.314	0.323	0.315	0.324	0.315	0.324	0.315±0.0004	0.324±0.0004

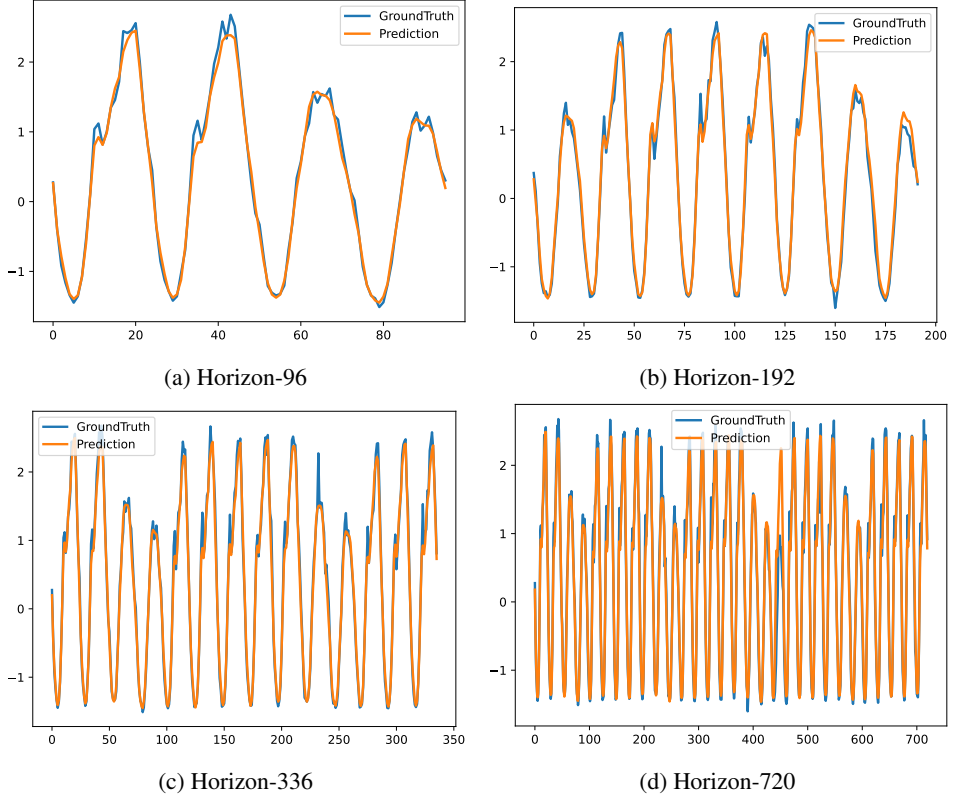


Figure 6: Prediction cases for the Traffic dataset with a look-back window length of  $l = 720$  and a forecast horizon of  $h \in \{96, 192, 336, 720\}$ .